

# INVESTIGATION INTO THE SOURCE OF SALINITY IN WATER SAMPLES FROM A COASTAL AQUIFER. CASE STUDY NINGO-PRAMPAM AREA, SOUTHERN GHANA.

Received: 6 May 2025

George Lutterodt

Accepted: 15 August 2025

Published: 30 September 2025

## Abstract

To contribute towards understanding the state of coastal groundwater resources in Ghana, this study employs field sampling, laboratory analysis, statistical and geochemical analysis to reveal the possible sources of mineralization/salinization in an unconfined gneissic aquifer in the eastern part of the Accra, Ghana. To do this, samples from 16 groundwater sources 11 shallow hand dug wells and 5 deep boreholes were sampled and analyzed for physical and chemical parameters. Ionic ratios involving chloride and other ratios ( $\text{Ca}^{2+}/\text{SO}_4^{2-}$ ,  $\text{Ca}^{2+}/\text{Mg}^{2+}$ ,  $\text{Ca}/(\text{HCO}_3 + \text{SO}_4)$ ), scatter plots:  $\text{Ca}/(\text{HCO}_3 + \text{SO}_4)$  and  $\text{Na}^+/\text{Cl}^-$  were employed to understand possible contribution of the sea to groundwater salinization. Geochemical tools were employed to understand various mechanisms responsible for salinization and hydrochemical water types. Results indicated that groundwater in the study area is saline with average EC values  $> 1\text{mS/cm}$  and water hardness ranging from moderately hard water to very hard water. The dominant ions (Na, Ca, Cl and  $\text{HCO}_3$ ) are implicated as the major determinants of mineralisation. Ionic ratios  $> 1$  for  $\text{Ca}^{2+}/\text{SO}_4^{2-}$ ,  $\text{Ca}^{2+}/\text{Mg}^{2+}$  and  $\text{Cl}/\text{HCO}_3$  and low ratios ( $< 1$ ) for  $\text{SO}_4^{2-}/\text{Cl}^-$ ,  $\text{K}^+/\text{Cl}^-$ , and  $\text{Mg}^{2+}/\text{Cl}^-$  indicate seawater in the aquifer. Observed hydrochemical water types: Na-Ca-Cl- $\text{HCO}_3$ , Na-Ca-Cl, Na-Cl and Na-Cl- $\text{HCO}_3$  confirm the influence of seawater in the aquifer. Base ion exchange processes influence the groundwater chemistry of almost all the samples (93.8%). Seawater intrusion in deep groundwater sources inferred from high mineralization of deep groundwater (depth  $> 20\text{ m}$ ) and high average Seawater mixing Index (SMI) of 1.2 in boreholes. Silicate weathering, evaporite dissolution and wastewater infiltration are additional processes contributing to salinization of the aquifer.

<sup>1\*</sup> University of Environment and Sustainable Development, Somanya, Eastern Region, Ghana,

\*Corresponding author: [glutterodt@uesd.edu.gh](mailto:glutterodt@uesd.edu.gh)

## Introduction

The crucial role groundwater resources play in the socio-economic development of many communities and settlements scattered across the World is indicated by the large number of countries that rely on aquifers for both rural and urban water supply. It is estimated that over 2.5 billion people worldwide (Shaji et al., 2021) out of the 8 billion people depend on groundwater as their sources of water for many uses including drinking.

In spite of its importance, groundwater available for many of its uses is under threat from poor quality and declining water table. Generally, natural and anthropogenic influences have been implicated for the poor groundwater quality worldwide (Rakib et al., 2022, Li et al., 2020), whereas the transient groundwater levels (rising and declining) in aquifers have been attributed to global warming (Visvalingam et al., 2024, Ostad-Ali-Askari et. al., 2019, Salimi et al., 2021). It is open knowledge that population growth coupled with increment in economic activities results in high demand for resources (e.g. Zhang et al., 2020) including water for its various uses.

As a result of rapid urbanization and industrialization within coastal areas (Visvalingam et al., 2024) a substantial fraction of the World's population live along coastlines (Wang et al., 2021, Kummu et. al., 2016, MacManus et al., 2021) which are regions stretching distances less than 100 km from the Coast (Idowu & Lasisi, 2020). Moreover, populations in these areas have been projected to increase (Maul & Duedall, 2019) in the coming years indicating a rise in water demand in these coastal regions. In many cases, coastal regions with high population densities rely on aquifers for their water needs (Basack et al., 2022), and indicate the importance of groundwater as a scarce freshwater resource in coastal communities (e.g. Ayeta et. al., 2024).

Major environmental challenge associated with groundwater use in coastal areas is the poor water quality due to high salinity and

contamination by nutrients and heavy metals together with microbial pathogens from anthropogenic sources; domestic and industrial wastewater and agricultural practices (Alorda-Kleinglass et al., 2024, Boumaiza et al., 2023; Malki et al., 2017, Ayeta et al., 2024, Lutterodt et al., 2021). Both the quality and quantity of groundwater available for use are affected by natural and anthropogenic influence including climate change (Rakib et al., 2022; Li et al., 2020, Macrae et al., 2013; Ostad-Ali-Askari et. al., 2019; Salimi et al., 2021).

Salinity is a measure of the total dissolved solids in water (Li et al., 2020) and is quantified by both the Total Dissolved Solids (TDS) in groundwater and its dependent physical quality parameter, the Electrical conductivity (EC). High salinity causes water shortage in coastal areas limiting availability of water for various purposes, and therefore affect the development of such areas (Wen et al., 2019). Both EC and TDS show groundwater affected by salinization (Jeen et al., 2021; Park et al., 2012; Rabinove, 1958). Salinization may be caused by seawater intrusion, evaporite dissolution, and wastewater infiltration. Jeen at al. (2021) and Rabinove (1958) have, respectively, indicated that EC values  $> 1$  mS/cm and TDS  $> 1000$  mg/l show groundwater affected by seawater intrusion and salinization.

In addition, water hardness is also used to infer mineralisation of groundwater. Water hardness is directly quantified based on magnesium and calcium content in water, and generally classified by the method of Sawyer and McCarthy (1967). From the classification, water hardness values of between 75-150 mg/l is considered moderately hard water, and 150 -300 mg/l r and water with hardness  $> 300$  mg/l are considered as hard water and very hard water, respectively. According to Li and co-workers (2020), more than 1 billion people in the world live in areas affected by saline

aquifers. Salinizations of coastal aquifers are caused by Seawater Influence (SWI) through two important processes; seawater intrusion and atmospheric sea aerosol deposition (Ganyaglo et al., 2017; Motevalli et al., 2018; Meira et al., 2007). Seawater intrusion is the lateral movement of seawater into fresh groundwater on the coast. The mechanisms and processes controlling seawater intrusion have variously been reviewed (Prusty & Farooq, 2020; Li et al. 2020). The reviews and other works published in the literature points out to natural and classical factors: e.g. hydraulic gradient and hydraulic connection between the sea and the coastal aquifers which are basic requirements for inland movement of seawater and local geological controls of groundwater occurrence (Prusty & Farooq, 2020), in addition to global climate change and sea-level rise. Sea aerosol deposition is also an important source of groundwater salinity in coastal aquifers, and are generated and transported by wind blowing towards land (Marks, 1990; Fitzgerald, 1991; Gong et al., 1997) and show their importance and contribution to the salinization of coastal aquifers. .

Improper water management practices, mainly over exploitation/abstraction of groundwater from coastal aquifers is an important factor causing seawater intrusion (Telahigue et al. 2020a). High groundwater abstraction due to population growth has been implicated by many researchers as a contributor to seawater intrusion into coastal aquifers (van camp et al., 2014, Manivannan and Elango, 2019). The process of over abstraction leads to a drop in fresh groundwater levels and reverses the hydraulic gradient causing inland movement of the sea. (Telhagigue tet al., 2018b).

Apart from indirect geophysical methods employed in the study and assessment of seawater intrusion (e.g. Asare et al., 2022), hydrochemistry and Hydrogeochemical methods (Telahigue et al., 2020a, b, Telahigue et al., 2018a, 2018b, Sunkari et al., 2021, Argamasilla et al., 2017, Abdalla,

2016, Rajendiran et al., 2021) have proved to be valuable in understanding the source of salinity in coastal aquifers. Due to the high chloride concentration in seawater and its unique tracer characteristics in groundwater environments, ionic ratios involving the ion has widely been used to assess seawater intrusion into coastal aquifer (Telahigue et al., 2018a,b , 2020a, Jampani et al., 2020, Slama & Bouhlila, 2017), with especially Br/Cl as an important indicator of seawater influence (Senthilkumar & Gnanasundar, 2021, Nair et al., 2016) due to the uniform concentrations of Br<sup>-</sup> and Cl<sup>-</sup> in seawater (Custodio & Herrera, 2000) and their good characteristics as tracers in groundwater environments (Acala & Custodio, 2008, Davis et al., 2004).

At present, more than 100 countries and regions in the world are threatened or affected by seawater intrusion ; Adyasari et al., 2019) Similarly in Ghana, there is growing evidence of the influence of the sea on groundwater in the coastal regions (Ganyaglo et al.2017, Lutterodt et al. 2021, Osiakwan et al., 2021, Asare et al., 2021, Darko et al., 2022), with the reasons for salinization unclear. Lutterodt et al. (2021) and Asare et al (2021) attribute their observations to seawater intrusion, whereas Ganyaglo et al. (2017) link their findings to sea aerosol deposition. Even though research into water has focused on groundwater in general, not much attention has been given to coastal aquifers (Ayeta et al. 2024). The Ningo-Prampram area is a coastal municipality in the Greater Accra Region of Ghana. The area is undergoing rapid urbanization, and evidenced by the rapid population growth in recent years (Obeng et al., 2015). Major climatic impacts have been reported in the area; both socio-economic and physical impacts due to sea level rise have been reported with coastal inundation and submersion, collapse of buildings due to the force of the sea and seawater intrusion (Darko et al., 2022). The forces of waves physically impact the coast, and frequently rise to greater heights

(Appeaning, 2011). Like many other communities in the country, the area suffers from irregular water flow in their pipes and tends to rely on other sources including groundwater (Ningo Prampram District Assembly Composite Budget Report 2023). To contribute towards understanding the state of coastal groundwater resources in Ghana, this work employs field sampling, laboratory analysis, statistical and geochemical analysis to reveal the possible sources of mineralization in the coastal aquifer of the Ningo-Prampram area in the eastern part of Accra, the capital of Ghana. The objectives of this study include the use of: physical water quality property EC/TDS and TH values to assess the salinization/mineralization of groundwater in the study area, ionic ratios involving chloride (Telahague et al., 2018, 2020, Jampani et al., 2020, Slama & Bouhlila, 2017) and other ionic ratios ( $\text{Ca}/\text{SO}_4$ ,  $\text{Ca}/\text{Mg}$ ,  $\text{Ca}/(\text{HCO}_3 + \text{SO}_4)$ ), scatter plots:  $\text{Ca}/(\text{HCO}_3 + \text{SO}_4)$  and  $\text{Na}/\text{Cl}$  to understand possible contribution of the sea to groundwater mineralization/salinization, geochemical tools to understand various mechanisms responsible for mineralization/salinization.

## Methods

### Study Area

Ningo and Prampram are two neighbouring peri-urban settlements located within the Ningo-Prampram district in the south eastern part of Accra plains of the Greater Accra Region of Ghana. The area is bordered on the south by the Atlantic Ocean (Figure 1). The area is characterised by coastal grassland and scrub vegetation interspersed with baobab trees. Relief is generally low, and slopes towards the sea with heights ranging from 5 m below sea level to about 60 m. The climate is characterized by two rainfall maxima. The major rainy season occurs between May and July and the minor wet season occurs between September and November. Mean annual rainfall ranges between 700 mm in the southern part of the district and increases

to 1220 mm in the Northern part with mean annual rainfall of 900 mm. The mean temperature is 26 C. (Dickson and Benneh, 1980). The Ningo-Prampram area forms part of the southeastern section of the Accra plains which are underlain by the Precambrian Dahomeyan rocks and the Togo formations. Migmatites and bands of acidic and basic gneisses and, quartzites, phyllites and schists, respectively form the Dahomeyan and Togo formations (Kesse, 1985). Groundwater occurrence in the Accra Plains restricted to discontinuities in the formations (Foppen et al., 2020). Near surface groundwater (depths < 10 m) is mainly controlled by weathering, weathering; the acidic rock types of the Dahomeyan weather to slightly permeable calcareous clay whereas the basic rocks weather

to impermeable clay (Junner & Bates 1945). Aquifers in the weathered zone can extend up to 25 m (Kortatsi, 2006), and are either semi-confined or unconfined (Foppen et al., 2020, Kortatsi, 2006).

Groundwater recharge in the plains is by rainfall (Kortatsi, 2006). Drainage pattern in the area is dendritic, the Akwapim Togo ranges which bounds the plains in the North is the source of rivers in the area. Surface water draining the area is the Dawhenya / Gyrokorgyor River which takes its source near Afienny. Sections of the river are silted due to their use as refuse dump (AFDB, 2008). The general pattern of drainage in the Ningo-Prampram district is dendritic with most of the streams taking their source from the Akwapim range which also serves as a watershed and flows in a northwest to southwest directions into lagoons on the coast. The people mainly practice Fishing and Trading in addition to farming. Water supply in the Ningo and Prampram area follows similar trends of unreliable water supply in other parts of the country (Obeng et al., 2015), communities within the district therefore rely on other sources for water, e.g. protected and unprotected boreholes, hand dug wells and springs, rivers and streams. They mostly rely on on-site

sanitation facilities to manage their excreta (Obeng et al., 2015).

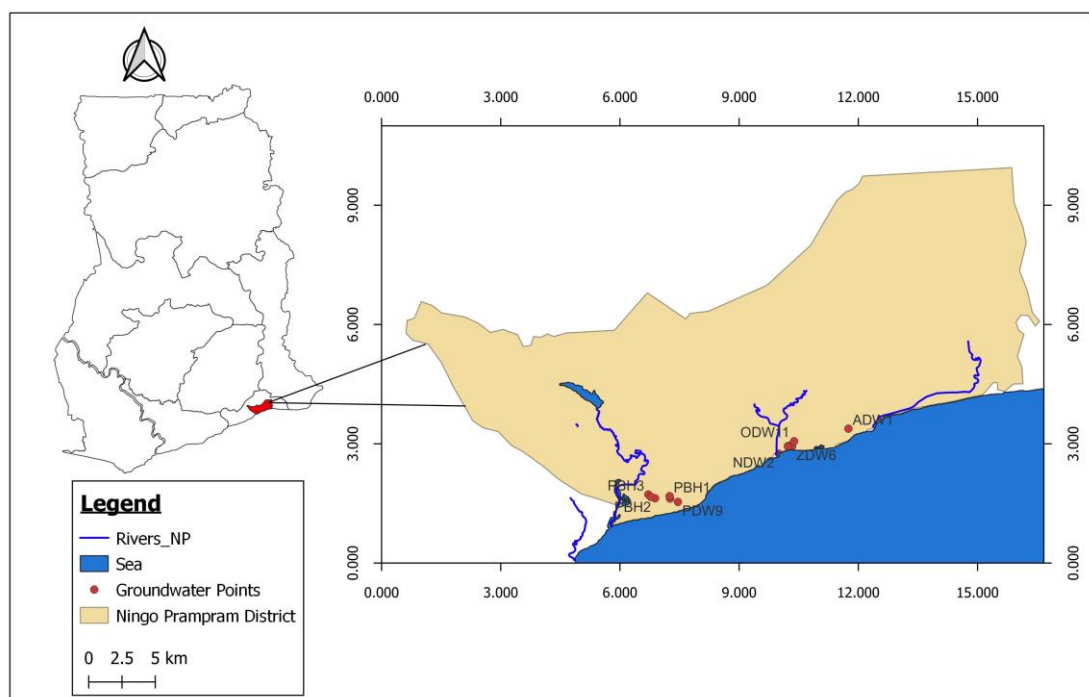


Figure 1: Location map of the Ningo-Prampram area showing groundwater points

### Field Sampling

Physico-chemical water quality field work was undertaken in December 2023 to characterise the hydrochemistry. Physical parameters: EC, TDS and pH were measured on site. TDS and EC were measured using a conductivity meter Cond340i (WTW GmbH, Weilheim Germany) calibrated at 25 °C and pH was determined using a pH meter pH340i (WTW GmbH, Weilheim Germany). Sixteen (16) groundwater points made up of 5 boreholes (BH) and 11 shallow hand dug wells (HDWs) were sampled for physical quality and hydro chemical characterisations of the aquifer. Two samples each of volume 250 mL were taken and filtered through 0.45 µm cellulose acetate filter (Whatman), into separate polystyrene bottles for major ion analysis. Samples for major cations (Na, Ca<sup>2+</sup>, Mg<sup>2+</sup>, K<sup>+</sup>) were acidified with 3 drops

of HNO<sub>3</sub> acid. All samples were placed in a cool box containing ice and transported to the laboratory of the National Nuclear Research Institute (NNRI) of the Ghana Atomic Energy Commission for hydrochemical analyses.

### Laboratory Analyses

The concentrations of the cations Na<sup>+</sup>, K<sup>+</sup>, Mg<sup>2+</sup> and anions SO<sub>4</sub><sup>2-</sup> and NO<sub>3</sub><sup>-</sup> were determined using Shimadzu Ion Chromatograph LC-20AD SP. Other parameters (Total hardness, Chloride and calcium concentrations) were determined via the use of analytical protocols described in the Standard Methods for the Examination of Water and Wastewater (APHA, 1998).

Total hardness (TH) and Ca<sup>2+</sup> amounts in the samples were titrimetrically determined using 25 ml of sample with a standard EDTA (Ethylene diamine tetra acetic acid) of concentration 0.01M. Ammonium buffer

and Eriochrome Black T (EBT) were used in TH determination whiles 1M NaOH solution and murexide indicator were used in  $\text{Ca}^{2+}$  determination and results expressed as mg/L. Chloride ( $\text{Cl}^-$ ) ion content was determined argentometrically using 25 ml of sample with 0.0141M  $\text{AgNO}_3$  (silver nitrate) as titrant and potassium chromate ( $\text{K}_2\text{CrO}_4$ ) as the indicator and the result reported in mg/L.

### Data Analyses

#### *Statistical summary, correlations between water quality parameters, piper plots and Ionic ratios*

Mixing with seawater, cation exchange processes, dissolution and precipitation reactions and wastewater infiltration are some of the processes known to influence salinity in groundwater. To identify possible mineralization processes of groundwater, a number of tools including statistical analysis; Statistical summary and correlation between chemical parameters involving relationship between Chloride as a tracer, EC and other water quality parameters, Piper's diagram (Piper, 1944), Chadha's diagram A plot between  $(\text{Ca} + \text{Mg}) - (\text{Na} + \text{K})$  and  $\text{HCO}_3 - (\text{SO}_4 + \text{Cl})$  applied to reveal the source of salinization in groundwater and gives four possible sources i.e. re-charge water ( $\text{Ca-HCO}_3$  type), reverse ion exchange ( $\text{Na-HCO}_3$ -type), seawater effect ( $\text{Na-Cl}$  type) and Base-ion exchange ( $\text{Ca-Mg-Cl}$  type) (Chadha, 1999).

Ionic ratios, mainly ion/chloride ratios and other ratios, scatter plots of  $\text{Na}^+/\text{Cl}^-$  vs  $\text{Ca}^{2+}/(\text{HCO}_3^{2-} + \text{SO}_4^-)$  (Abdalla, 2016) and Na normalized molar ratios after Gaillardet et al., (1999) are used to characterized water samples, understand the various geochemical processes occurring, reveal the dominant ion exchange processes and understand the sources of ions in the aquifer. Scatter plot of  $\text{Cl}^-/\text{HCO}_3^-$  as a function of chloride concentration is applied to understand the possible effect of seawater on groundwater samples from the wells.

### *Seawater Mixing Index*

A modified form of the Seawater Mixing Index (SMI) by Sinclair (1974) and Park et al. (2005) was employed to evaluate the degree of mixing of groundwater and seawater (Bhagat et al., 2021, and Park et al., 2005). The SMI is based on the concentrations of four major ionic components (Na, Cl, Mg and  $\text{SO}_4$ ) in Ocean and given by the equation below:

$$SMI = a \frac{C_{Na}}{T_{Na}} + b \frac{C_{Mg}}{T_{Mg}} + c \frac{C_{Cl}}{T_{Cl}} + d \frac{C_{SO_4}}{T_{SO_4}} \quad (1)$$

where the a, b, c, and d, are constants and reflect the relative concentration proportion of  $\text{Na}^+$ ,  $\text{Mg}^{2+}$ ,  $\text{Cl}^-$ , and  $\text{SO}_4^{2-}$  in seawater, respectively ( $a=0.31$ ,  $b=0.04$ ,  $c=0.57$ ,  $d=0.08$ ); C is measured concentration (mg/l), T is the regional threshold values of the respective ions. In this work, T is determined by plotting ionic concentrations (mg/l) against cumulative probabilities. The cumulative probability curves are fitted with a third order polynomial, points of inflection are obtained by the second differential of the concentration with respect to the cumulative probability to obtain the T values. SMI value  $> 1$  indicate seawater mixing with groundwater.

### *Chloro-alkaline Indices*

Possible occurrence of base ion exchange between groundwater and the solid rock was assessed by using the chloralkaline indices which involves two equations:

$$CAI - I = \frac{Cl - (Na + K)}{Cl} \quad (2a)$$

$$CAI - II = \frac{Cl - (Na + K)}{(\text{SO}_4 + \text{HCO}_3 + \text{NO}_3)} \quad (2b)$$

Direct base ion exchanges of  $\text{Na}^+$  and  $\text{K}^+$  in the fluid phase with  $\text{Ca}^{2+}$  and  $\text{Mg}^{2+}$  in the solid rock is inferred when the CAI-I&II values are negative, for positive values, the exchange occurring is reverse and indirect



(Schoeller, 1965, Zhang et al., 2021, Mahmoudi et al., 2017).

## Results and discussions

### Physical parameters

Statistical summary of measured water quality parameters for hydrochemical characterisation are presented in Table 1. EC values ranged from 842.0  $\mu\text{S}/\text{cm}$  to 10.78  $\text{mS}/\text{cm}$  with a mean of 2,693.8  $\mu\text{S}/\text{cm}$ , TDS 463.5 to 5929.0  $\text{mg}/\text{l}$  mean 1481.5  $\text{mg}/\text{l}$ , mean values of EC and TDS are comparatively higher in deep groundwater, i.e. BH (5.3  $\text{mS}/\text{cm}$  and 2917  $\text{mg}/\text{l}$ ) than in shallow HDWs (2.85  $\text{mS}/\text{cm}$  and 1567  $\text{mg}/\text{l}$ ), four boreholes and a HDW recorded TDS values higher than the maximum of 1500  $\text{mg}/\text{l}$  for fresh water (Rabinove, 1958). Results of average concentrations of anions, cations and values of physical quality parameters (TDS, TH and EC) implies that groundwater in the study area is mineralised, with higher mineralisation in deep groundwater compared to water samples from shallow hand dug wells (Table 1) The higher average EC/TDS values can be attributed to the influence of the sea due to the nearness of the groundwater sources (HDWs and BHs) to the sea. Both EC and TDS values have been used as indicators of salinization (Jeen et al., 2021, Park et al., 2012, Rabinove, 1958) EC values  $> 1 \text{ mS}/\text{cm}$  may reflect Seawater intrusion into coastal aquifers (Jeen et al., 2021), in this work, the EC of all groundwater sources were  $> 1 \text{ mS}/\text{cm}$  with the exception of two shallow HDWs with values  $< 1 \text{ mS}/\text{cm}$  (ECs of 0.98  $\text{mS}/\text{cm}$  and 0.84  $\text{mS}/\text{cm}$ , for wells KDW 10 and ZDW8, respectively) and can be considered as fresh based on the classification of Park et al. (2012). Average values of TDS in both groundwater sources ( $> 1000 \text{ mg}/\text{L}$ , Table 1) confirms the salinization of groundwater according to the classification by Rabinove, (1958). High values of the EC and TDS in the boreholes can be attributed to the intrusion of high-density seawater at lower levels in the aquifer in addition to the possibility of long residence time of groundwater in deeper levels. The assertion

of SWI is attributable to the high average concentrations of anions and cations, and also higher TDS/EC and TH in deep groundwater sources (BHs) compared to shallow groundwater (HDW). This points out to the possible inflow of dense seawater at lower depths into the aquifer through forced convection due to groundwater over exploitation (Vallejos et al., 2020, Vengosh and Rosenthal, 1994.). Groundwater conditions showed neutral to near alkaline with pH varying between 7.85 to 8.99 and an average of 8.53. Average pH in HDWs and BHs are respectively, 8.6 and 8.3. The alkaline nature of groundwater in the area has been observed within similar coastal aquifers (e.g. Moorthy et al., 2024, Bourjila et al., 2024, Lutterodt et al., 2021, Abdalla, 2016). In the current work, the near neutral to alkaline nature of groundwater is attributable to the possible inflow of seawater (Lutterodt et al., 2021), dissolution of seashells and calcareous materials within the beach sands in addition to the possible infiltration of wastewater from the surface.

Total Hardness (TH) values were between 112.1  $\text{mg}/\text{l}$  to 1232.3  $\text{mg}/\text{l}$  and a mean of 373.7  $\text{mg}/\text{l}$ . Computed average TH is higher in BH (544  $\text{mg}/\text{l}$ ) than in HDW (296  $\text{mg}/\text{l}$ ). Based on classification of water hardness (Sawyer and McCarthy, 1967), hardness test for samples from all 5 BHs and one HDW (43.8%) indicated very hard water (i.e.  $\text{TH} > 300 \text{ mg}/\text{l}$ ). For the rest of the HDWs, three (18.8%) are moderately hard (75-150  $\text{mg}/\text{l}$ ), Six (6). 37.5% hard water (150-300  $\text{mg}/\text{l}$ ). The observed hardness can be attributed to high concentrations of Ca and Mg from seawater.

From the EC/TDS values and TH it is concluded that all groundwater sources are mineralised, with hardness water ranging from moderately hard water to very hard water. Mineralisation is higher in deep groundwater than hand dug wells.

### *Ions contributing to salinization/mineralization*

From Table 1, it can be concluded that the order of concentration of anions and cations, respectively, follow  $\text{Cl}^- > \text{HCO}_3^- > \text{PO}_4^{2-} > \text{NO}_3^- > \text{SO}_4^{2-}$  and  $\text{Na}^+ > \text{Ca}^{2+} > \text{Mg}^{2+} > \text{K}$  and show high chloride and sodium content in water samples. Generally, average concentrations of the ions are higher in BHs compared to the shallow HDWs. The high  $\text{Na}^+$  and  $\text{Cl}^-$  content can be attributed to the proximity of the wells to the sea (Telahague et al., 2018a, Nair et al., 2020) note that all groundwater points sampled are at short distances from the sea ( $< 2$  km). A number of workers (e.g. Telahague et al., 2018a, b, Bhagat et al., 2021) have linked the abundance of Na and Cl in groundwater in coastal aquifers to seawater intrusion. The observed wide variation in Cl (mean 428.8, SD 564.3) and Na (Mean 270.8, SD 334.3) in shallow groundwater (HDW) compared to the deeper boreholes (BH) (Na: mean

769.4, SD 265.7, Cl: mean 1181.8, SD 455.9) (Table 1), may indicate additional sources of  $\text{Cl}^-$  and  $\text{Na}^+$  input apart from direct seawater influence. Silicate weathering (Shin et al., 2020) and possible leachate of wastewater from improper wastewater management facilities e.g. sullage drains and rubbish dumps may be the additional sources of ion input into shallow groundwater (e.g. Jeen et al., 2021). In addition, the overall strong correlation between  $\text{Na}^+$  and  $\text{Cl}^-$  ( $r = 0.99$ ) is an indication that two ions are released from sources with equivalent concentrations of the two ions (e.g. halite, seawater, domestic salt). High standard deviations of  $\text{Na}^+$  and  $\text{Cl}^-$  in HDWs indicate shallow groundwater chemistry in the study area may be affected by additional factors including rock weathering (Shin et al., 2020) and infiltration of wastewater from on-site sanitation facilities (Lutterodt et al., 2021).

Table 1: Statistical summary of physical and chemical quality parameters of samples from groundwater points: (Hand dug wells (HDW) and Boreholes (BH). All units in Mg/l unless given

Parameters	HDW				BH				Average (HDW and BH)
	min	max	Mean	SD	min	max	mean	SD	
EC ( $\mu\text{S}/\text{cm}$ )	842.8	2850.0	1568.4	655.9	2450.0	10780.0	5304.0	3291.6	2735.7
TDS (mg/l)	463.5	1567.5	862.6	360.7	1347.0	5929.0	2917.0	1810.6	1504.6
pH (-)	8.1	9.0	8.6	0.3	7.9	8.5	8.3	0.3	8.5
Ca	32.1	346.3	82.7	89.6	121.5	223.8	164.2	42.9	108.2
Mg	4.8	89.2	22.0	23.1	17.3	51.4	32.1	13.4	25.2
Na	48.3	1242.3	270.8	334.3	396.5	1100.0	769.4	265.7	426.6
K	0.9	3.8	2.4	1.0	2.7	3.6	3.1	0.4	2.6
Cl	106.0	2099.0	428.8	564.3	499.9	1736.2	1181.8	455.9	664.1
$\text{NO}_3$	7.2	69.5	36.4	19.4	23.3	53.0	42.3	12.0	38.2
$\text{PO}_4$	28.5	189.8	73.5	48.1	79.0	123.0	96.3	18.4	80.6
$\text{HCO}_3$	84.0	648.0	239.7	161.8	306.0	444.0	379.0	51.6	283.3
TH (mg/l)	112.1	1232.3	296.3	316.3	395.2	630.8	544.1	92.7	373.7
$\text{SO}_4$	7.1	47.4	18.4	12.0	19.7	30.8	24.1	4.6	20.2

The concentrations of  $\text{HCO}_3^-$  and  $\text{Ca}^{2+}$  ions as the second dominant ions in the aquifer can be attributed to fresh groundwater recharge, in addition, the presence of calcareous shells in the aquifer might have contributed to the  $\text{HCO}_3^-$  in the samples, a

similar observation was made by Raja and Co-workers (2021) In addition, seawater is known to contain higher concentrations of the two ions. The strong correlation ( $r = 0.92$ ) between the  $\text{HCO}_3^-$  and  $\text{Ca}^{2+}$  ions (Table 2) supports the observation.



Additionally, weathering of primary minerals in the gneissic rock types of the area might have contributed to the Ca in groundwater. This assertion is supported by the near neutral to alkaline pH of the samples due to Ca-enrichment. Observed high SD of Ca and  $\text{HCO}_3^-$  content in HDW (Table 1) can also be attributed to a possibility of diverse sources of input of the ions. For  $\text{Ca}^{2+}$ , sources may include mineral dissolution in the saprolite of the shallow zones and wastewater infiltration, with  $\text{HCO}_3^-$  content linked to groundwater recharge in the shallow zones. Low deviation of the concentrations of the ions ( $\text{HCO}_3^-$  and  $\text{Ca}^{2+}$ ) from the mean in samples from the BHs may be due to limited sources of input and can be ascribed to the possible intrusion of seawater with more stable ionic concentrations at lower levels, and also explains the higher  $\text{Ca}^{2+}$  concentration in BHs than in HDWs. According to Kumar et al. (2014) high concentrations of  $\text{Mg}^{2+}$  in a coastal aquifer may be an indication of seawater intrusion, in this work, Mg ranks as the third most abundant Cation in groundwater of the area contribution may be coming from effect of the sea and also dissolution of minerals containing the magnesium ion. Low Nitrate content can be attributed to (Lutterodt et al., 2021). The low potassium content in the aquifer may be

due to its adsorption to clay minerals (Sarin et al., 1989), note that the aquifer is predominantly made up of the Dahomeyan gneisses that weather into clay mineral, in addition groundwater occurrence in the shallow gneisses are controlled by weathering (Foppen et al., 2020) which produces clayey soils. It is difficult to explain the low sulfate content in the water samples, for the ion is one of the major components in seawater. It is speculated that sulfate ions may be undergoing precipitation and or sorption by the positive clay minerals of the area.

Scatter plots of sum of cations against major cations ( $\text{Na}^+$ ,  $\text{Ca}^{2+}$ ,  $\text{Mg}^{2+}$  and  $\text{K}^+$ ) and also sum of anions against the anions ( $\text{Cl}^-$ ,  $\text{HCO}_3^-$ ,  $\text{PO}_4^{3-}$  and  $\text{SO}_4^{2-}$ ) and correlation analyses of measured water quality parameters (Table 2) and (Figure 2), were used to, respectively, understand the contribution of specific ions to mineralization of groundwater and the sources of mineralization (Telahague et al., 2020). Results indicate a strong correlation between sum of cations and  $\text{Na}^+$  ( $R^2 = 0.91$ ), and also for  $\text{Ca}^{2+}$  ( $R^2 = 0.91$ ), and an almost perfect correlation ( $R^2 = 0.99$ ) was observed between the dominant anion  $\text{Cl}^-$  and sum of anions. The results confirm the dominance of  $\text{Na}^+$ ,  $\text{Ca}^{2+}$ , and  $\text{Cl}^-$  in the aquifer.

Table 2; Correlation matrix of physico-chemical parameters. Substantially large correlation coefficients ( $r \geq 0.7$ ) are in bold.

	<i>pH</i>	<i>EC</i>	<i>TDS</i>	<i>Cl</i>	<i>SO<sub>4</sub></i>	<i>HCO<sub>3</sub></i>	<i>NO<sub>3</sub></i>	<i>PO<sub>4</sub></i>	<i>Na</i>	<i>K</i>	<i>Ca</i>
<b>EC</b>	-0.64										
<b>TDS</b>	-0.64	<b>1.00</b>									
<b>Cl</b>	-0.61	<b>0.87</b>	<b>0.87</b>								
<b>SO<sub>4</sub></b>	<b>-0.86</b>	<b>0.79</b>	<b>0.79</b>	<b>0.73</b>							
<b>HCO<sub>3</sub></b>	-0.44	<b>0.89</b>	<b>0.89</b>	<b>0.83</b>	0.60						
<b>NO<sub>3</sub></b>	-0.29	0.49	0.49	0.50	0.32	0.62					
<b>PO<sub>4</sub></b>	-0.57	0.23	0.23	0.28	0.53	0.26	0.14				
<b>Na</b>	-0.59	<b>0.85</b>	<b>0.85</b>	<b>0.99</b>	<b>0.71</b>	<b>0.85</b>	0.52	0.32			
<b>K</b>	-0.34	0.57	0.57	0.59	0.54	<b>0.79</b>	0.40	0.32	0.61		
<b>Ca</b>	-0.60	<b>0.97</b>	<b>0.97</b>	<b>0.92</b>	<b>0.77</b>	<b>0.92</b>	0.46	0.31	<b>0.91</b>	0.65	
<b>Mg</b>	-0.65	<b>0.85</b>	<b>0.85</b>	<b>0.70</b>	<b>0.70</b>	<b>0.81</b>	0.65	0.38	<b>0.69</b>	0.52	<b>0.81</b>

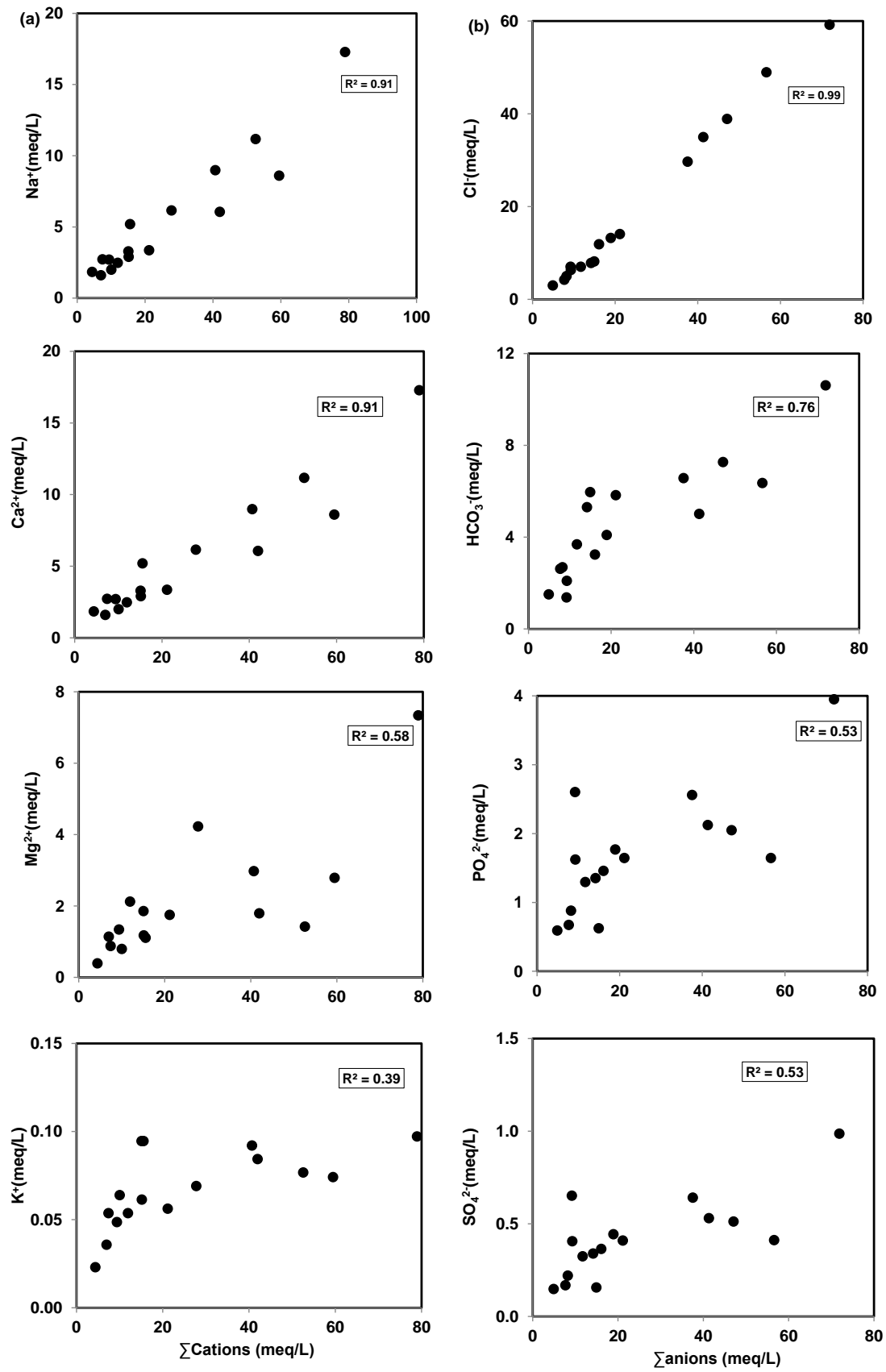


Figure 2: Association between (a)  $\Sigma$  cations and  $\text{Na}^+$ ,  $\text{Ca}^{2+}$ ,  $\text{Mg}^{2+}$  and  $\text{K}^+$  (meq/L) and (b)  $\Sigma$  Anions and  $\text{Cl}^-$ ,  $\text{HCO}_3^-$ ,  $\text{PO}_4^{2-}$  and  $\text{SO}_4^{2-}$

Also,  $\text{HCO}_3^-$  showed a good correlation with sum of anions ( $R^2=0.76$ ). The observation is an indication that the dominant ions ( $\text{Na}^+$ ,  $\text{Ca}^{2+}$  and  $\text{Cl}^-$ ) are responsible for the mineralization of the Ningo-Prampram Aquifer. The observed low correlation between sum of cations and  $\text{Mg}^{2+}$  ( $R^2 = 0.58$ ), and between sum of anions and  $\text{PO}_4^{2-}$  and  $\text{SO}_4^{2-}$  both with  $R^2 = 0.53$  show moderate contribution to the mineralization process of the aquifer. The correlation matrix (Table 2) reiterates the observed relationship between EC/TDS and other chemical parameters known to be related to dissolved solids (*Cl*:  $r = 0.87$ , *SO<sub>4</sub>*,  $r = 0.79$ , *HCO<sub>3</sub>*,  $r = 0.89$ , *Na*,  $r = 0.85$ , *Ca*:  $r = 0.97$ , *Mg*:  $r = 0.85$ ). Results support the mixing of seawater with fresh groundwater in addition to cation exchange processes within the aquifer systems, this assertion is linked to the strong correlation

between EC and with major components of seawater ( $\text{Cl}^-$ ,  $\text{Na}^+$ , and  $\text{Mg}^{2+}$ ) and cations released into the groundwater systems either through base exchange processes ( $\text{Ca}^{2+}$  and  $\text{Mg}^{2+}$ ), dissolution of rock-minerals and or infiltration of wastewater from the surface.

The results indicate that ions in groundwater of the area may be due to contribution from multiple sources, likely SWI, dissolution of rock minerals and infiltration of wastewater and mineralization of the aquifer is due to the higher concentrations of the dominant cations  $\text{Na}^+$  and  $\text{Ca}^{2+}$  and major anions  $\text{Cl}^-$  and  $\text{HCO}_3^-$ .

#### Base Exchange processes

Figure 3 show the occurrence of both direct and reverse base ion exchanges, respectively, in seven (7 i.e. 3 BHs and 4 HDWs) and eight (8 2 BHs and 6 HDWs) of the samples .

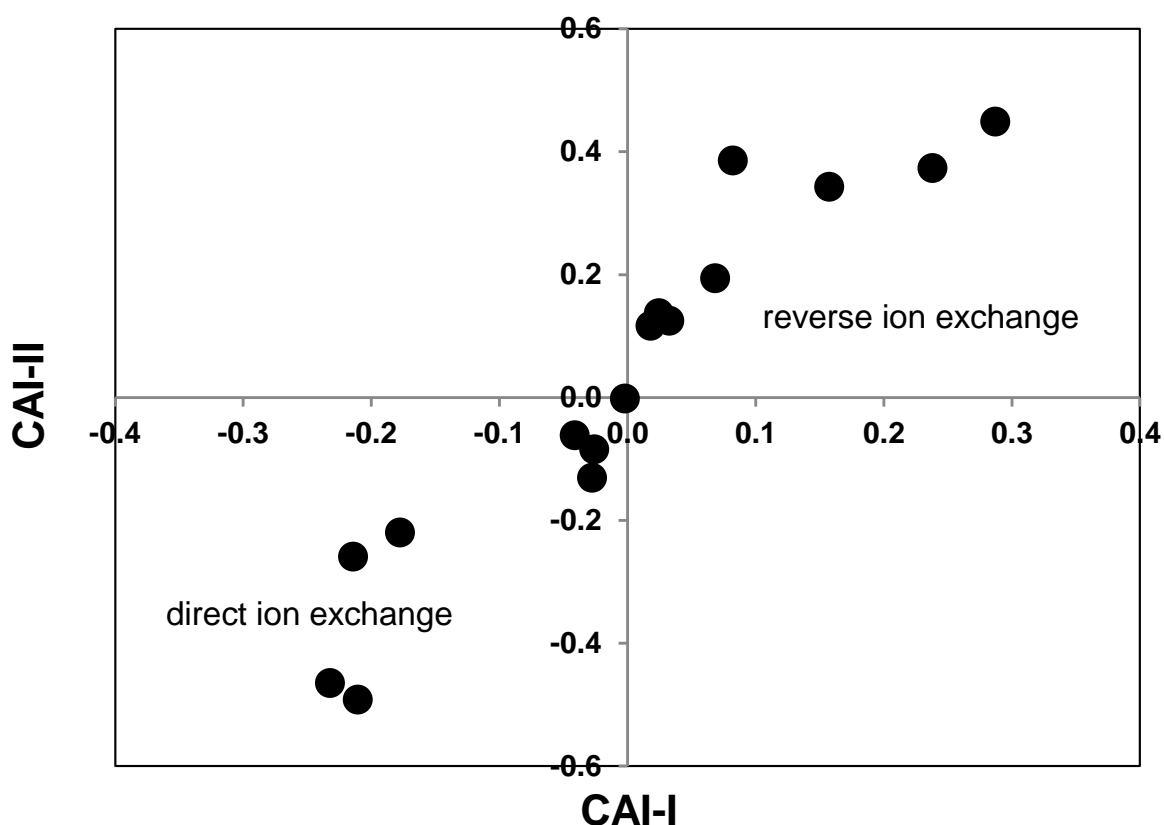


Figure 3: Chloro-Alkaline indices showing reverse ion exchange and direct ion exchange.

For one sample from a HDW (PWD9) there seem to be no net effect of Base Exchange processes, and can be attributed to the possibility of equal rates of direct and indirect exchanges. Base ion exchange processes are therefore independent of the depth of groundwater sources. Both mechanisms might have occurred via the introduction of saline water into the aquifer via atmospheric aerosol deposition and seawater intrusion. From the results it can be concluded that in addition to the base exchange processes mixing between seawater and recharge and or fresh groundwater might have occurred. It can be concluded that base ion exchange processes influence the groundwater chemistry of almost all the samples (93.8%).

### *Ionic ratios*

Like many other workers (Asare et al., 2021, Sunkari et al., 2021, Hajj et al., 2021, Telahague et al., 2018, 2020) ionic ratios (Table 3) involving ions with high concentrations in seawater was used as index to assess the influence of seawater on the samples. In addition, ionic ratios as a function of Chloride (salinity) concentration (meq) were used to understand and infer the possible mixing of seawater and freshwater. It is important to note that ionic ratios are also useful in revealing water-rock interaction processes (Kura et al., 2014), wastewater infiltration and other process that alter ionic concentrations and influence the chemistry of groundwater.

Salinization of coastal fissure groundwater in the Ningo-Prampram area, southern Ghana.

Results show that for all samples, values of ratios  $\text{Ca}^{2+}/\text{SO}_4^{2-}$ ,  $\text{Ca}/\text{Mg}$  and  $\text{Cl}^-/\text{HCO}_3^-$  were all greater than 1 and Cl dominance showed in the ratios  $\text{SO}_4/\text{Cl}$  and  $\text{Mg}^{2+}/\text{Cl}^-$  with all values  $< 1$  and  $\text{K}^+/\text{Cl}^- < 0.02$ . The reported ratios have variously been used to indicate seawater intrusion into coastal aquifers ( $\text{Mg}^{2+}/\text{Cl}^- < 1$ : Al-Qurnawy et al., 2023, Asaer et al., 2021,  $\text{K}/\text{Cl} < 0.02$ : Asare et al., 2021, Jones et al. 1999, Vengosh and Rosenthal., 1994,  $\text{Ca}^{2+}/\text{Mg}^{2+} > 1$ , Bear et al.,

1999) In this work, the low values of ion/chloride ratios ( $< 1$ ) confirms the dominance of  $\text{Cl}^-$  in groundwater of the area (Jones et al. 1999) with the sea as the possible source of  $\text{Cl}^-$  due to its nearness to the groundwater sources sampled for the study ( $< 5$  km from the Coast) (Al-Qurnawy et al., 2023, Hajj et al. 2021, Telahague et al., 2018, 2020). Possible pathways for seawater influence (SWI) on groundwater in the area may be through seawater intrusion and atmospheric aerosol deposition. The low values of the ion/chloride ratios in BHs compared to shallow HDW (Table 3) is an indication of high influence of the chloride sources at deeper groundwater level and this may be attributed to seawater intrusion.

Results showed that deep groundwater (depth  $> 20$  m) sources are more mineralized compared to shallow groundwater and reflected in the higher average values of molar ratios (meq) (e.g.  $\text{Ca}^{2+}/\text{Mg}^{2+}$ ,  $\text{Cl}^-/\text{SO}_4^{2-}$ ,  $\text{Ca}^{2+}/\text{SO}_4^{2-}$ ,  $(\text{Ca}^{2+}+\text{Mg}^{2+})/\text{Cl}^-$ ,  $(\text{Ca}^{2+}+\text{Mg}^{2+})/(\text{HCO}_3^{2+}+\text{SO}_4^{2-})$  in the boreholes compared to HDW. Low average values of  $\text{Ca}/\text{Na}$  and  $\text{Ca}/\text{Cl}$  in BHs (Table 3) were also obtained. The observation is attributable to seawater intrusion in deep groundwater due to its dissolved constituents, and also the possibility of long residence time of deep groundwater might have contributed to the higher mineralisation.

For all samples  $\text{Ca}^{2+}/\text{SO}_4^{2-} > 1$  with high ratios in BHs (11.42 to 21.8, average 16.62) compared to shallow groundwater sources (3.07 to 21.03, average 11)  $\text{Ca}^{2+}/\text{SO}_4^{2-} > 1$  has been attributed to Seawater influence/Intrusion (Asare et al., 2021). The non-correlation between  $\text{Ca}^{2+}/\text{SO}_4^{2-}$  and  $\text{Cl}^-$  concentration (Figure 4d) may be an indication of a complex combination of processes determining the concentrations and fate of  $\text{Ca}^{2+}$  and  $\text{SO}_4^{2-}$  in groundwater of the area.  $\text{SO}_4$  may be undergoing sorption processes on clayey soils as speculated earlier with additional input of  $\text{Ca}^{2+}$  from wastewater in addition to contributions from

Base Exchange processes contributing to removal and addition of  $\text{Ca}^{2+}$  to the fluid phase from the solid aquifer.

Computed  $\text{Na}^+/\text{Cl}^-$  values indicated similar concentrations in meq with average value of 1 for both HDW and BHs, indicating these ions may be emanating from similar sources e.g. seawater, deposited sea aerosol, halite dissolution and anthropogenic influence from on-site sanitation facilities. Note that the influence of seawater on coastal aquifers results in Na: Cl ratio of 0.86 or less (Telahigue et al., 2020a, Bear et al., 1999). In this work, 13 out of the 16 samples have  $\text{Na}^+/\text{Cl}^-$  ratios  $> 0.86$  (see figure 4a.) and give an indication of additional sources of Na input into groundwater of the area. In addition, the non-correlation between Na/Cl as function of salinity confirms the possible multiple sources of Na in groundwater of the area. The observation can be linked to rock weathering (Jena et al., 2024), contribution from wastewater infiltration

and mixing of seawater and groundwater. Wide variation of Na and Cl content in groundwater of the area confirms the possible multiple sources.

For all samples results indicate  $\text{Ca}^{2+}/\text{Mg}^{2+} > 1$ . According to Bear et al. (1999) this result could indicate Ca enrichment in both shallow groundwater and the deeper boreholes. Average values in BH (3.76)  $>$  that of HDW (2.53 (Table 3).  $\text{Ca}^{2+}/\text{Mg}^{2+}$  ratio has variously been used as an important natural tracer of seawater intrusion in coastal aquifers (Pulido-Leboeuf et al., 2003, Ouhamdouch et al., 2021). A combination of processes might have contributed to the  $\text{Ca}^{2+}/\text{Mg}^{2+} > 1$ . At high water hardness, Mg prevents the precipitation of  $\text{Ca}^{2+}$  in groundwater (Juarez et al, 2023). In this work, all water sampled showed water hardness with more than 80% of the samples (13 sampling points) showing hard water to very hard water.

Table 3: Summary of Ionic ratios computed in Meq and Base Exchange Index (BEX) from respective parameters for HDW and BH and combined averages.

Ionic ratios	HDW				BH				Avg (HDW and BH)
	Min	Max	mean	SD	Min	Max	mean	SD	
Na/Cl	0.71	1.21	0.98	0.17	0.96	1.23	1.03	0.11	1.00
Mg/Cl	0.10	0.30	0.18	0.07	0.04	0.30	0.11	0.11	0.15
K/Cl	0.002	0.012	0.008	0.003	0.002	0.005	0.003	0.001	0.006
Cl/SO <sub>4</sub>	10.82	60.00	28.56	14.99	34.38	118.80	68.28	32.59	40.97
Ca/Cl	0.24	0.66	0.40	0.14	0.17	0.44	0.28	0.11	0.36
(Ca+Mg)/Cl	0.34	0.80	0.58	0.16	0.22	0.74	0.38	0.21	0.52
NO <sub>3</sub> /Cl	0.02	0.16	0.07	0.04	0.01	0.06	0.03	0.02	0.06
Cl/HCO <sub>3</sub>	1.37	5.58	2.80	1.47	2.42	7.70	5.39	2.09	3.61
HCO <sub>3</sub> /Na	0.19	0.72	0.46	0.20	0.13	0.23	0.17	0.04	0.38
Ca/Mg	1.17	4.68	2.55	1.18	1.46	7.85	3.76	2.41	2.93
Ca/SO <sub>4</sub>	3.07	21.03	11.00	5.31	11.42	21.80	16.62	4.51	12.76
Ca/Na	0.21	0.87	0.44	0.21	0.18	0.36	0.26	0.08	0.38
Ca/(HCO <sub>3</sub> +SO <sub>4</sub> )	0.54	1.49	0.89	0.28	0.99	1.43	1.21	0.17	0.99
(Ca+Mg)/(HCO <sub>3</sub> +SO <sub>4</sub> )	0.84	2.12	1.28	0.35	1.42	1.68	1.61	0.11	1.38

This might have led to Ca-enrichment as  $\text{Mg}^{2+}$  may be preventing  $\text{Ca}^{2+}$  from precipitation; the strong positive correlation ( $r = 0.81$ ) supports this assertion. Most importantly, base exchange analysis

indicate that 7 out of the sixteen samples are influenced by direct ion exchange process involving exchange of  $\text{Ca}^{2+}$  and  $\text{Mg}^{2+}$  on solid aquifer with Na from the fluid phase. Values of  $\text{Ca}^{2+}/\text{Mg}^{2+} > 1$  may indicate



seawater intrusion (Sudaryanto and Naily, 2018, Carol and Kruse, 2012, Carol and Kruse, 2009, Sudaryanto and Naily, 2018) with high ratios ( $> 2$ ) and low ratios ( $\text{Ca}^{2+}/\text{Mg}^{2+}, \leq 2$ ), respectively, showing additional input from silicate mineral weathering and calcareous mineral

weathering (Abu et al., 2024). Strong positive correlation between  $\text{Ca}^{2+}$  and  $\text{Mg}^{2+}$  ( $r = 0.81$ ) may indicate higher fraction of the ions emanate from the same source mainly direct ion exchange and possibly wastewater.

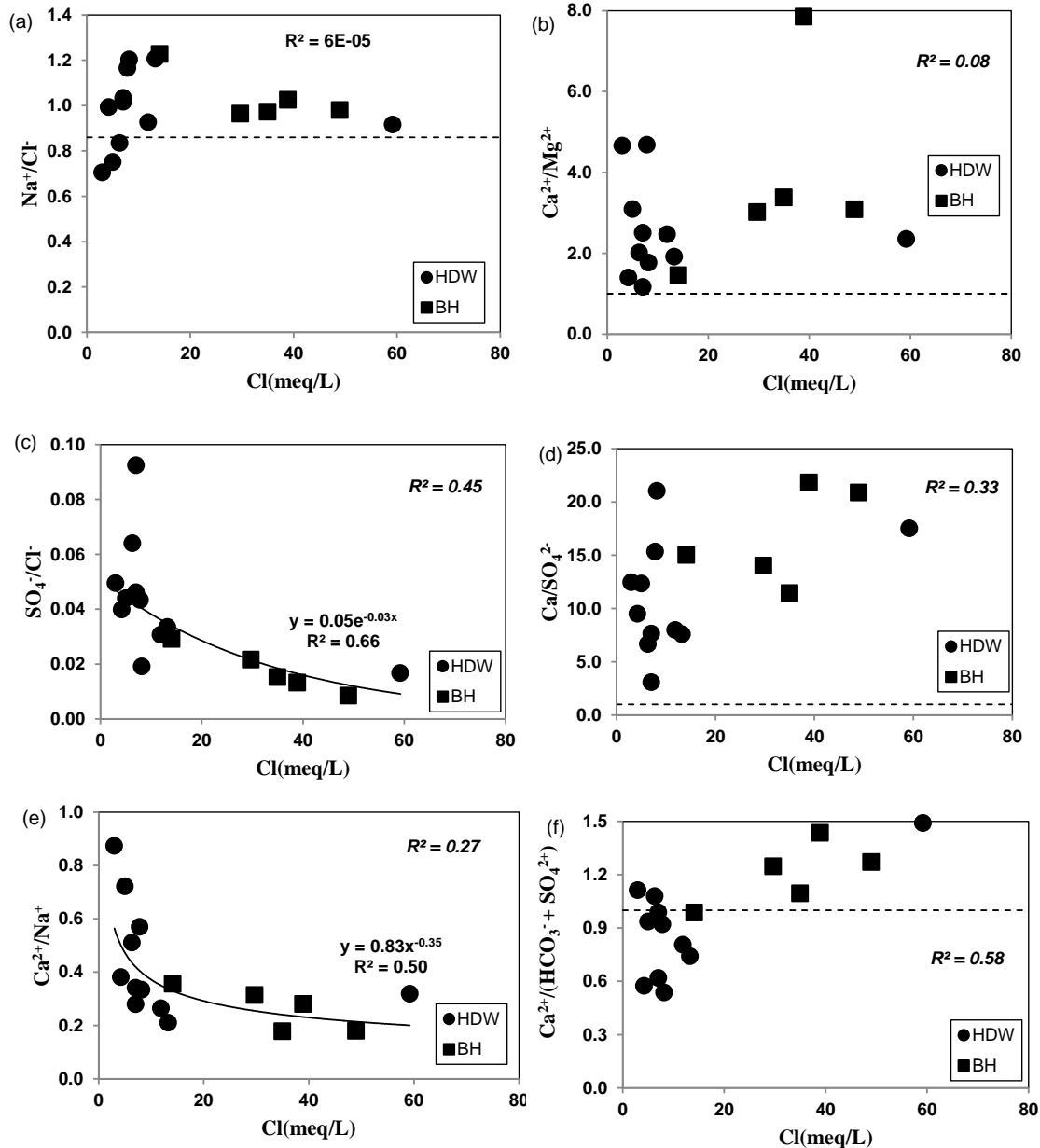


Figure 4: Scatter plots of ionic ratios: (a)  $\text{Na}^+/\text{Cl}^-$  (b)  $\text{Mg}^{2+}/\text{Ca}^{2+}$  (c)  $\text{SO}_4^{2-}/\text{Cl}^-$  (d)  $\text{Cl}^-/\text{HCO}_3^-$  (e)  $\text{Ca}^{2+}/\text{Na}^+$  (f)  $\text{Ca}^{2+}/(\text{HCO}_3^- + \text{SO}_4^{2-})$  as a function of  $\text{Cl}^-$  (meq):

Scatter plot of  $\text{Ca}^{2+}/\text{Mg}^{2+}$  as a function of salinity (Cl) (Figure 4b) did not show any correlation and may indicate that mixing with seawater may not be the main source of

the  $\text{Ca}^{2+}$  and  $\text{Mg}^{2+}$  in groundwater of the area.

More than half of the samples (56%) show  $\text{Ca}^{2+}/(\text{HCO}_3^- + \text{SO}_4^{2-}) > 1$ , (Figure 4f) and

include all deep groundwater sources sampled and three of HDWs, the result can be linked to seawater intrusion (Klassen et al, 2014, Carol and Kruse, 2012, El Moujabber et al., 2006, Sudaryanto and Naily, 2018). Also,  $\text{SO}_4^{2-}/\text{Cl}^-$  as a function of salinity indicated an exponential ( $R^2 = 0.7$ ) (See figure 4c) reduction with increasing salinity indicating that the low  $\text{SO}_4^{2-}$  content in the aquifer may be coming from other sources. This observation is similar to the findings of Paulido-Leboeff, et al. (2003) who observed a power law reduction in the ratio with increasing fraction of seawater.

Dominance of Na in groundwater of the area is confirmed by low values (ratios <1) of Ca/Na and  $\text{HCO}_3^-/\text{Na}$  (Table 3), both ratios ( $\text{Ca}^{2+}/\text{Na}^+$  and  $\text{HCO}_3^-/\text{Na}^+$ ) are important indicators of mineralization due to water-rock interactions, silicate and carbonate weathering and evaporite dissolution (Ruiz-Pico et al., 2019; Xu et al., 2022). Na dominance can be traced to multiple processes including indirect Base Exchange releasing  $\text{Na}^+$  and  $\text{K}^+$  into

groundwater as noted earlier and also mixing of groundwater with seawater.

$\text{Ca}^{2+}/\text{Na}^+$  as a function of salinity ( $\text{Cl}^-$ ) (Figure 4e) did not show a linear correlation ( $R^2=0.27$ ) but indicated a power law ( $R^2=0.50$ ) reduction in the ratio with increasing salinity confirming multiple sources of input of the two minerals into the aquifer system with fractional input from seawater for both. The plots of the Na- normalized molar ratios (Gaillardet et al., 1999) i.e. the relationship between  $\text{HCO}_3^-/\text{Na}$  versus  $\text{Ca}^{2+}/\text{Na}^+$ , and  $\text{Mg}^{2+}/\text{Na}^+$ , versus  $\text{Ca}^{2+}/\text{Na}^+$  (Figure 5) were used to contribute towards understanding of the sources of mineralization. The importance of the relationships is linked to the fact that ratios are neither affected by any of the physical processes; dilution, flow rate, dilution and evaporation and therefore the Hydrochemical origin of the ions can be traced (Zhang et al., 2023). In figure 5 (a and b) the plots cluster within the evaporite (Seawater) region. The observation can be largely attributed to seawater influence via intrusion and atmospheric sea aerosol deposition and the dissolution of evaporite minerals that may be present in the aquifer.

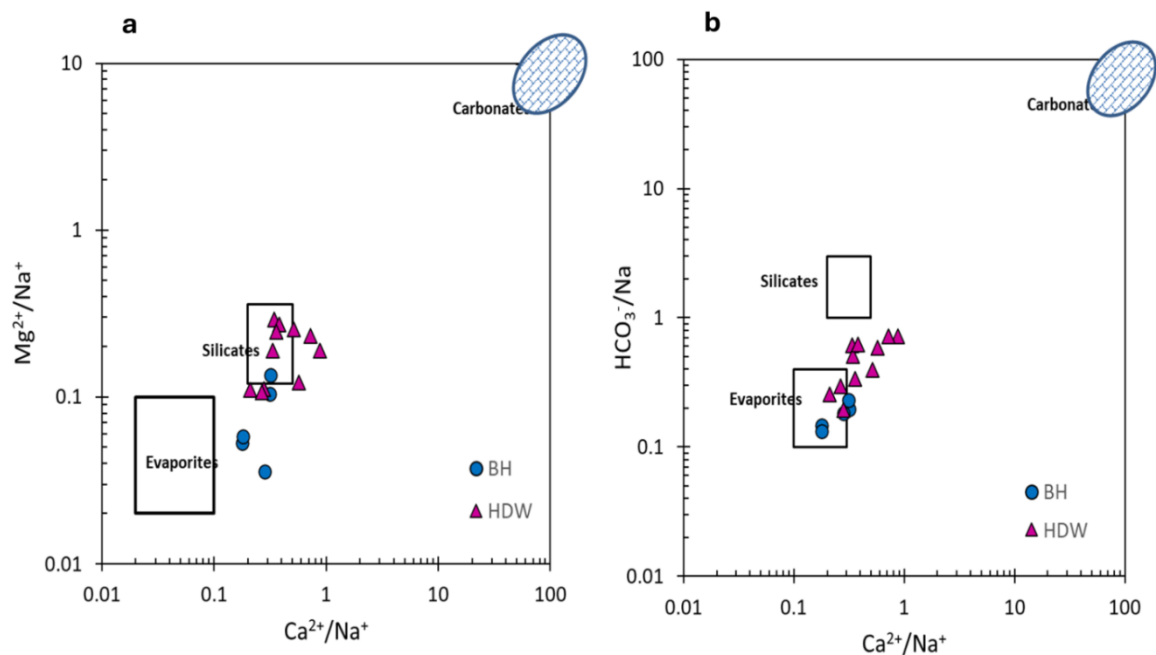


Figure 5; Na normalized molar ratios after Gaillardet et al. (1999) showing the relationship between (a)  $\text{HCO}_3^-/\text{Na}^+$  and  $\text{Ca}^{2+}/\text{Na}^+$  and (b)  $\text{Mg}^{2+}/\text{Na}^+$  and  $\text{Ca}^{2+}/\text{Na}^+$

The presences of data points in the silicate region, particularly in Figure 6a, indicate interactions with silicate minerals that release magnesium, further influencing groundwater chemistry. The low presence of data in the carbonate zone could indicate either the limited presence of carbonate

minerals in the aquifer materials or a geochemical environment where the dissolution of carbonate minerals is not the dominant geochemical process compared to evaporite dissolution and silicate weathering.

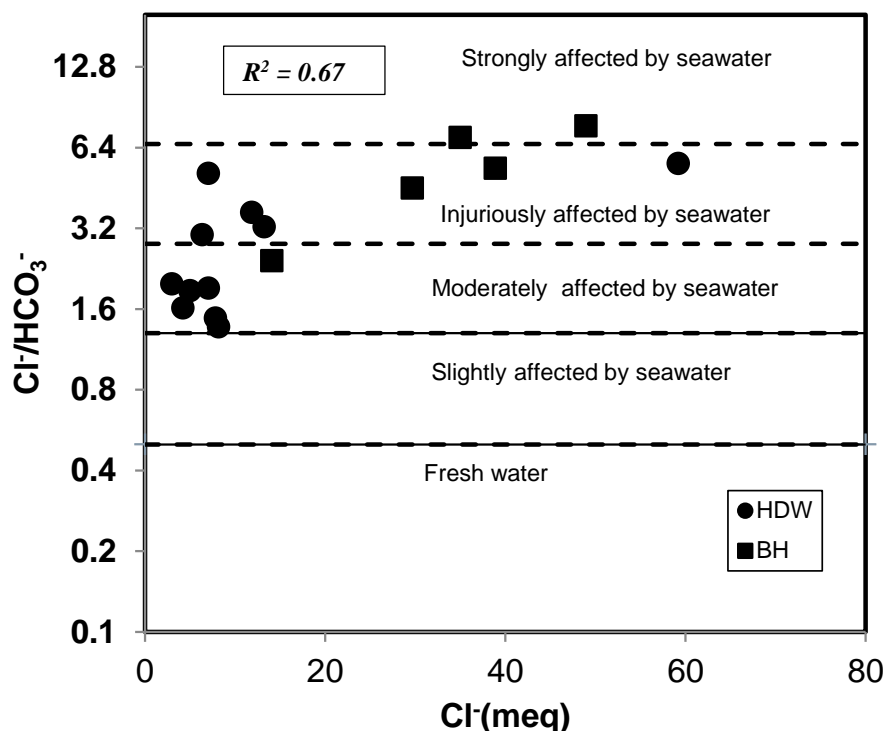


Figure 6: Hydrochemical facies distribution based on  $Cl/HCO_3^-$  as a function of  $Cl^-$ .

A modified form of the Simpson's ratio,  $Cl^-/HCO_3^-$  as a function of  $Cl^-$  has proved to be an important tool in the classification of groundwater affected by seawater (Todd, 1959, Revelle, 1941 and Raja et al., 2021). Computed values for  $Cl^-/HCO_3^-$  were all  $> 1$ , with an average value of 3.61 indicating an influence by the sea (Al-Qurnawy et al., 2023, Shin et al., 2020, Revelle, 1941).  $Cl^-/HCO_3^-$  as a function of  $Cl^-$  is employed to classify samples from the groundwater sources (Figure 6); Seven (43.8%) of the samples from HDW recorded ratios  $1.3 < Cl^-/HCO_3^- < 2.8$  (Figure 6) indicating moderate effect of seawater, seven shallow HDW and 2 BHS are injuriously and strongly affected by seawater, respectively (Shin et al., 2020, Revelle, 1941). The strong effect of the seawater on deep

boreholes can be attributed to seawater intrusion (El Moujabber et al., 2006).

Both Chadha's diagram (Figure 4a) and the relation between the ratios  $Ca^{2+}/(HCO_3^- + SO_4^{2-})$  and  $Na^+/Cl^-$  (Figure 7b) (Chadha, 1999, Abdalla, 2016, Agoubi et al., 2014) have proved to be useful in characterizing water types and understanding ion exchange processes in aquifers. From Chadha's diagram all samples are influenced by seawater (Na-Cl water type). The observation is attributable to the dominant  $Cl^-$  and  $Na^+$  ions in the water samples coming from the sea's strong influence on the aquifer through encroachment (Abdalla, 2016) and deposition of sea aerosols due to the nearness of the wells and boreholes to the sea. Scatter plots of  $Ca^{2+}/(HCO_3^- + SO_4^{2-})$  against  $Na^+/Cl^-$  (Figure 7b) reveals that six groundwater sources (1 BH and 5 HDWs)

and 3 HDWs, respectively have Ca-excess and Chloride excess indicating that 56 % of the groundwater sources are influenced by

seawater. The rest of the sources (2 HDW and 3 BHs) have Calcium excess (Ca-excess) and a single BH in a natural state

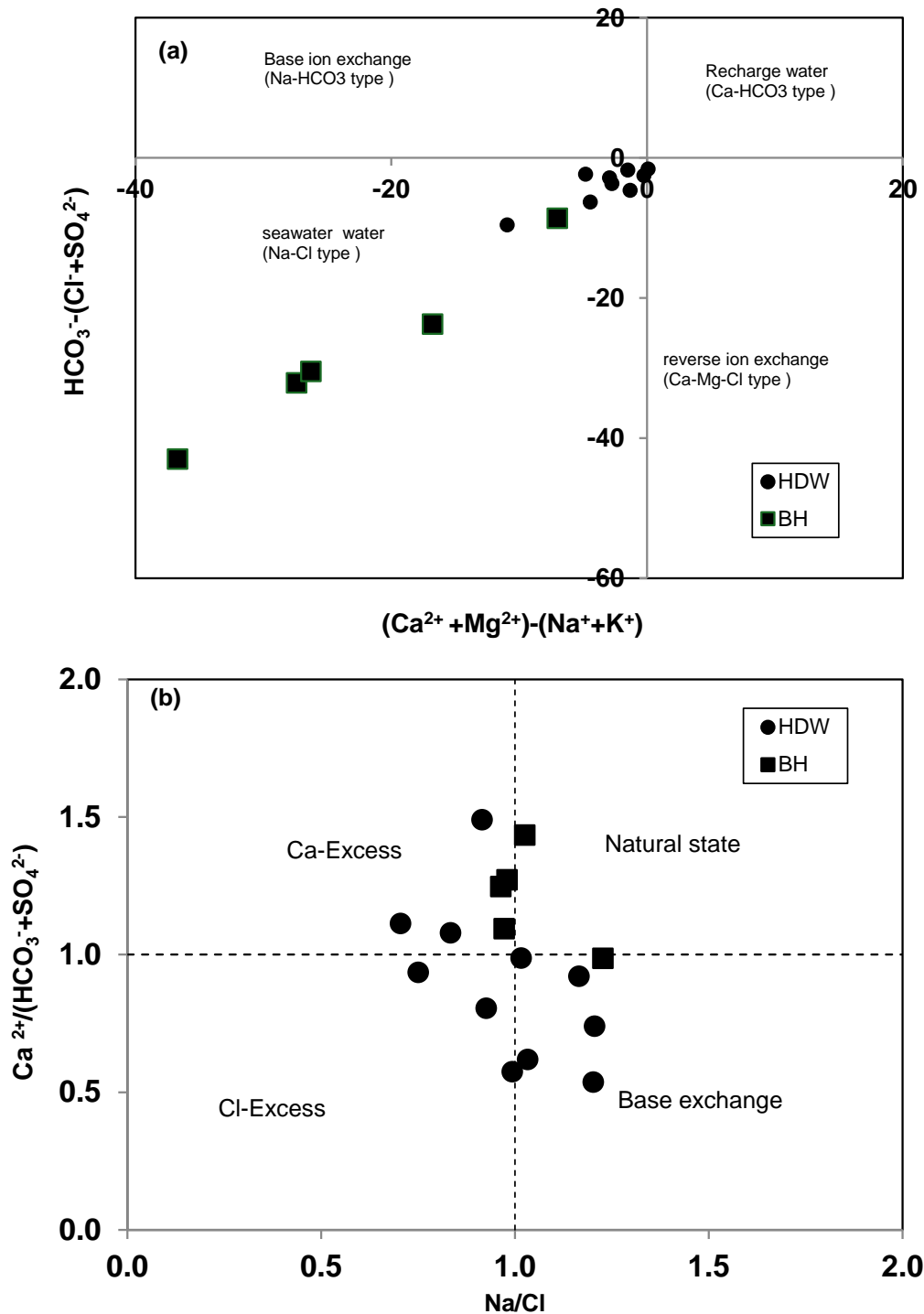


Figure 7: (a) Chadha plot showing salinization of the aquifer (b) Scatter plot of  $\text{Ca}/(\text{HCO}_3 + \text{SO}_4)$  against  $\text{Na}/\text{Cl}$  showing possible geochemical processes in the aquifer.

From ionic ratios ( $\text{Ca}^{2+}/\text{SO}_4^{2-}$ ,  $\text{Ca}^{2+}/\text{Mg}^{2+}$  and  $\text{Cl}^-/\text{HCO}_3^-$ ) values  $>1$  and for low values of ratios  $\text{SO}_4^{2-}/\text{Cl}^-$ ,  $\text{K}^+/\text{Cl}^-$ , and

$\text{Mg}^{2+}/\text{Cl}^-$  all  $<1$ , the Na-Cl water type produced from the Chadha's diagram it is concluded that seawater has influenced

groundwater in the area. Based on  $\text{Ca}^{2+}/(\text{HCO}_3^- + \text{SO}_4^{2-}) > 1$  and the scatter plot between  $\text{Ca}^{2+}/(\text{HCO}_3^- + \text{SO}_4^{2-})$  and  $\text{Na}^+/\text{Cl}^-$  it is concluded that 56% of the samples are influenced by the sea. From high average ratios for  $\text{Ca}^{2+}/\text{SO}_4^{2-}$ ,  $\text{Ca}^{2+}/\text{Mg}^{2+}$  and  $\text{Cl}^-/\text{HCO}_3^-$  and much lower values all in BHs compared to shallow HDW seawater intrusion is inferred in deep boreholes (depth > 20 m). Silicate weathering, evaporite dissolution and infiltration of wastewater contribute to mineralization of the aquifer.

### Hydrochemical facies Evolution

Piper plots shown in figure 8 give four (4) main water types in the area and reflect distinct ion combinations. The common water types observed are Na-Ca-Cl- $\text{HCO}_3$  (8 HDW), Na-Ca-Cl (3BHs), Na-Cl (2 BHs and 1 HDW) and Na-Cl- $\text{HCO}_3$  (2 HDW) and respectively represent 50%, 18.75%, 18.75% and 12.5% of the samples. The five deep groundwater sources are characterized by Na-Ca-Cl (3) and Na-Cl (2) water types with the rest of the water types observed in shallow hand dug wells.

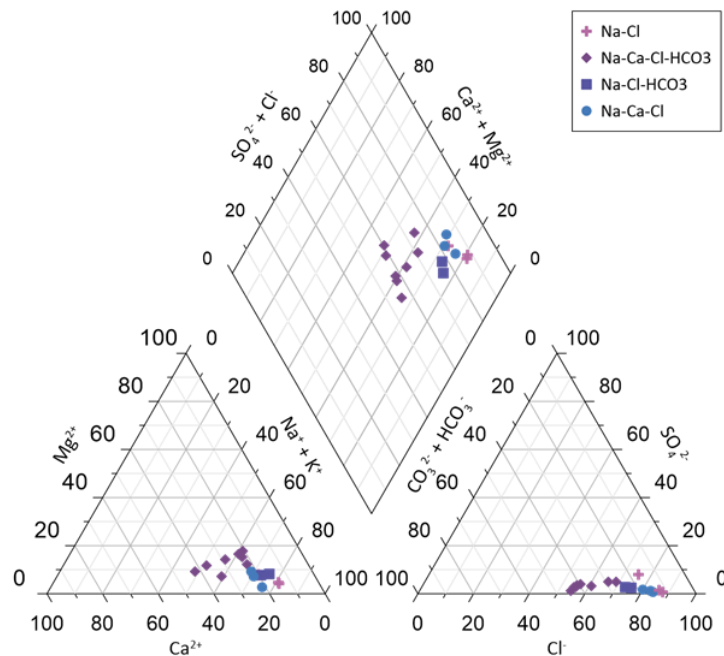


Figure 8: Piper plots showing four distinct classes/types of water in the Ningo-Prampram area

The observed common Na-Ca-Cl- $\text{HCO}_3$  water type in the shallow zone (<10 m depth) can be attributed to a mixture of higher fractions of saline water produced from dissolution of deposited sea aerosols and dissolution of carbonate rocks and recharge low fractions of fresh groundwater with  $\text{Ca}^{2+}$  and  $\text{HCO}_3^-$  content produced from rock-water interaction and dissolution of material from the saprolites of the aquifer. Seawater facies-Na-Cl, observed in a HDW and 2 BHs may be due to the possibility of two different processes; for HDW a combination of upconing of seawater inflow

due to groundwater abstraction creating a forced convection in addition to contribution of sea aerosol from the surface and for the BH lateral intrusion of the seawater at deeper groundwater levels may be implicated (Mao et al., 2021). Boreholes characterized by intrusion facies-Na-Ca-Cl (Raja et al., 2020) may represent a mixture of different water sources mainly seawater intrusion and multiple geochemical processes e.g. initial cation exchange process between Na from seawater and Ca from the solid aquifer material followed by saturation by seawater. Na-Cl- $\text{HCO}_3$  water



types could be the result of ion exchange processes, carbonate dissolution, mixing of recharge water with seawater and/or silicate weathering.

### Seawater Mixing Index

Figure 9 show cumulative probability curves for ions, and show inflections points

and threshold concentrations of the ions ( $\text{Na} = 598.2 \text{ mg/l}$ ,  $\text{Mg} = 32.1 \text{ mg/l}$ ,  $\text{Cl} = 976.5 \text{ mg/l}$  and  $\text{SO}_4 = 21.8 \text{ mg/l}$ ), which differentiate samples with seawater mixing effect in the study area (Park et al., 2005). SMI values for all shallow groundwater sources (HDW) was  $< 1$  with the exception of ODW11 (SMI=2.2) and all BHs had SMI values  $> 1$  with the exception of PBH1 (SMI= 0.6).

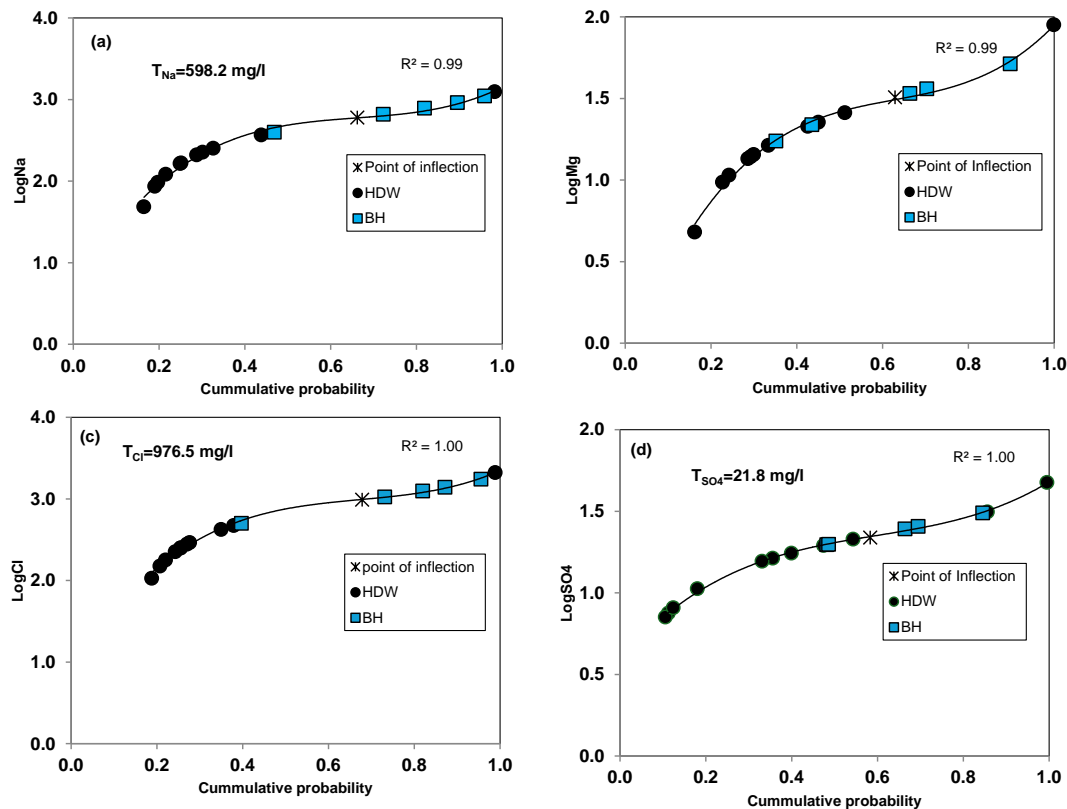


Figure 9: Cumulative probability curves for (a) Na (b) Mg (c) Cl and (d)  $\text{SO}_4$  showing the point of inflection determined from the second differential of the third order polynomial obtained from the relation between the concentrations and cumulative probabilities

Again, results confirm a greater influence of the sea in deep groundwater within the study area with average SMI value of 1.2 for the BHs, mixing might have been caused by intrusion as previously explained. Average SMI value for HDW was 0.5. The high SMI value of HDW ODW11 may be due to a combination of Hydrogeochemical processes including upwelling of seawater due to abstraction and also infiltration of wastewater from the surface.

### Summary and Conclusions

In this case study, physical and chemical quality of groundwater samples from shallow ( $< 10 \text{ m}$  deep) hand dug wells (HWDs) and boreholes (BHs) (Depths  $> 20 \text{ m}$ ), were respectively analyzed in the field and laboratory. The limited sample size of the boreholes, and the methodological limitation of the inability to analyse for Br- in water samples are potential limitations associated with the study. However, the complex combination of geochemical tools

used in the analyses of the results and the distinctly high values of the physical and chemical parameters in borehole samples associated with highly mineralised seawater validates interpretation and findings of the work.

Table 4: Summary of water characteristics in relation to effect by seawater using various methods factor's likely to influence salinity of groundwater in the area

Well ID	Source	Geology	Water Type Piper plot	Depth (m)	Distance from the sea (Km)	Interpretation from Chad da's diagram	CAI-I & II (Base exchange)	Ca/(HCO <sub>3</sub> <sup>+</sup> SO <sub>4</sub> ) vrs Na/Cl	SMI	Effect by seawater (Cl/HCO <sub>3</sub> )	EC
ADW 1	HDW	Gneiss	Na-Cl	8.2	0.94	SWE	Reverse	Base exchange	0.4	Inj. affected	1209.0
NDW 2	HDW	Gneiss	Na-Ca-Cl-HCO <sub>3</sub>	4.3	0.41	SWE	Reverse	Base exchange	0.3	Mod. affected	1970.0
ZDW 3	HDW	Gneiss	Na-Ca-Cl-HCO <sub>3</sub>	2.2	0.35	SWE	Reverse	Base exchange	0.3	Mod. affected	1870.0
ZDW 4	HDW	Gneiss	Na-Ca-Cl-HCO <sub>3</sub>	2.2	0.34	SWE	Direct	Ca-excess	0.3	Mod. affected	1240.0
ZDW 5	HDW	Gneiss	Na-Ca-Cl-HCO <sub>3</sub>	1.36	0.31	SWE	reverse	Base exchange	0.3	Mod. affected	1530.0
ZDW 6	HDW	Gneiss	Na-Cl-HCO <sub>3</sub>	1.6	0.31	SWE	Direct	Cl-excess	0.5	Inj. affected	1215.0
ZDW 7	HDW	Gneiss	Na-Cl-HCO <sub>3</sub>	1.7	0.31	SWE	Reverse	Base exchange	0.6	Inj. affected	2510.0
ZDW 8	HDW	Gneiss	Na-Ca-Cl-HCO <sub>3</sub>	1.4	0.28	SWE	Direct	Ca-excess	0.1	Mod. affected	842.8
PDW 9	HDW	Quartzite	Na-Ca-Cl-HCO <sub>3</sub>	3.2	0.69	SWE	No reaction	Cl-excess	0.2	Mod. affected	1032.0
KDW 10	HDW	Quartzite	Na-Ca-Cl-HCO <sub>3</sub>	4.7	1.12	SWE	Direct	Cl-excess	0.2	Mod. affected	983.1
ODW 11	HDW	Quartzite	Na-Ca-Cl-HCO <sub>3</sub>	5.14	0.71	SWE	Direct	Cl-excess	2.2	Mod. affected	2850.0
PBH 1	BH	Quartzite	Na-Ca-Cl	>20	1.30	SWE	Reverse	Base exchange	0.6	Mod. affected	10780.0
PBH 2	BH	Quartzite	Na-Ca-Cl	>20	1.33	SWE	Reverse	Natural state	1.4	Inj. affected	5820.0
PBH 3	BH	Quartzite	Na-Ca-Cl	>20	1.74	SWE	Direct	Ca-excess	1.1	Inj. affected	3830.0
PBH 4	BH	Quartzite	Na-Cl	>20	1.53	SWE	Direct	Ca-excess	1.2	strongly affected	2450.0
PBH 5	BH	Quartzite	Na-Cl	>20	1.30	SWE	Direct	Ca-excess	1.7	strongly affected	3640.0

Statistical summary of physical quality parameters, EC/TDS and TH were used to infer salinization/mineralization of the aquifer and correlation matrix, geochemical tools including ionic ratios and scatter plots, Seawater Mixing Index (SMI), chloro-alkaline indices, and hydrochemical facies evolution were used to understand the possible geochemical and geohydrological processes controlling the hydrochemistry of the aquifer.

From the results it is concluded that :

A summary of results of key geochemical processes and characteristics obtained at individual groundwater points are presented in Table 4.

- Groundwater in Ningo-Prampram area is saline with average EC values > 1mS/cm , and water samples show moderately hard water to very hard water.
- Salinity is mainly caused by higher concentrations of dominant cations (Na<sup>+</sup> and Ca<sup>2+</sup>) and dominant anions (Cl<sup>-</sup> and HCO<sub>3</sub><sup>-</sup>)
- Aquifer is influenced by seawater through mixing processes and inferred

from : ionic ratios  $>1$  for  $\text{Ca}^{2+}/\text{SO}_4^{2-}$ ,  $\text{Ca}^{2+}/\text{Mg}^{2+}$  and  $\text{Cl}/\text{HCO}_3^-$  and low ratios ( $<1$ ) for  $\text{SO}_4/\text{Cl}$ ,  $\text{K}^+/\text{Cl}^-$ , and  $\text{Mg}/\text{Cl}$  all for all water samples.

- Seawater (Na-Cl water type) for all samples on Chadda's diagram and the dominance of Na and Cl in all the water types (Na-Ca-Cl- $\text{HCO}_3$ , Na-Ca-Cl, Na-Cl and Na-Cl- $\text{HCO}_3$ ) revealed by hydrochemical facies evolution.
- Base ion exchange processes influence the groundwater chemistry of almost all the samples (93.8%).

## References

- Abdalla, F. (2006). Ionic ratios as tracers to assess seawater intrusion and to identify salinity sources in Jazan Coastal aquifer, Saudi Arabia. *Arab J. Geosci* 9, 40
- Abdul-Wahab, D., Adomako, D., Abass, G., Adotey, D.K., Anornu, G., & Ganyaglo, S., (2020). Hydrogeochemical and isotopic assessment for characterizing groundwater quality and recharge processes in the Lower Anayari catchment of the Upper East Region, Ghana. *Environ. Dev. Sustain.*
- Abu, M., Zango, M.S., & Kazapoe, R.W. (2024). Controls of groundwater mineralization assessment in a mining catchment in the Upper West Region, Ghana: Insights from hydrochemistry, pollution indices of groundwater, and multivariate statistics. *Innovation and Green Development* 3, 100099.
- Adjabeng, M.J., Frimpong, J.A., Couston-Appiah, W., Afarid, E., Ampofo, W., & Richard Adanu, R. (2023). Risk Factors for Influenza Disease in Shai-Osudoku and Ningo-Prampram Districts in the Greater Accra Region of Ghana *International Journal of TROPICAL DISEASE & Health* 44, 1-13.
- Adyasari D., Hassenruck C., Oehler T., Sabdaningsih A., & Moosdorf N. (2019). Microbial community structure associated with submarine groundwater discharge in northern Java (Indonesia). *Sci. Total Environ.* 689, 590–601. doi: 10.1016/j.scitotenv.2019.06.193, PMID:
- Seawater intrusion might have occurred in deep groundwater sources and inferred from Higher mineralization of deep groundwater (depth  $> 20$  m) and high average Seawater Mixing Index (SMI) of 1.2 in boreholes
  - Silicate weathering, evaporite dissolution and wastewater infiltration contribute to the salinization of the aquifer.
- Africa Development Bank Group (2015). Environmental and Social Impact Assessment summary. Partial Risk guarantee program in support of gas to power. Project No P-GH-F00-008.
- Agoubi, B., Kharroubi, A., & Abida, H. (2014). Geochemical Assessment of Environmental Impact on Groundwater Quality in Coastal Arid Area, South Eastern Tunisia. *Journal of Environmental Science and Engineering Technology*, 2, 35-46.
- Akoto, O., Teku, J.A., & Gasinu, D. (2019). Chemical characteristics and health hazards of heavy metals in shallow groundwater: case study Anloga community, Volta Region, Ghana. *Applied Water Science*, 9, 36.
- Alcalá, F.J., & Custodio, E. (2008). Using the Cl/Br ratio as a tracer to identify the origin of salinity in aquifers in Spain and Portugal. *Journal of Hydrology*, 359, 189-207.
- Alorda-Kleinglass, A., Rodellas, V., Diego-Feliu, M., Marba, N., Morell, C., & Garcia-Orellana, J. (2024). The connection between Submarine Groundwater Discharge and seawater quality: The threat of treated wastewater injected into coastal aquifers. *Science of the Total Environment* 922, 170940.

- Al-Qurnawy, L. S., Almallah, I. A., & Alrubaye, A. (2023). Identification of Seawater Intrusion in the Dibdibba Coastal Aquifer, South of Iraq Using Chemical Indicators and Multivariate Analyses. *IOP Conf. Ser.: Earth Environ. Sci.* 1215 012054
- APHA (1998). *Standard Methods for the Examination of Water and Wastewater*. 20th Edition, American Public Health Association, American Water Works Association and Water Environmental Federation, Washington DC.
- Appaning, K. A., Larbi, L., Amisigo, B., & Ofori-Danson, P. K. (2011). Impacts of coastal inundation due to climate change in a CLUSTER of urban coastal communities in Ghana. *West Africa. Remote Sensing*, 3(9), 2029–2050.  
<https://doi.org/10.3390/rs309202>
- Argamasilla, M., Barberá, J.A., & Andreo, B., (2017). Factors controlling groundwater salinization and hydrogeochemical processes in coastal aquifers from southern Spain. *Sci. Total Environ.* 580, 50–68.
- Asare, A., Appiah-Adjei, E.K., Owusu-Nimo, F., & Bukari Ali (2022). Lateral and vertical mapping of salinity along the coast of Ghana using Electrical Resistivity Tomography: The case of Central Region, *Results in Geophysical Sciences*, 12, 100048, ISSN 2666-8289.
- Asare, A., Appiah-Adjei, E.K., Ali, B., & Owusu-Nimo, F. (2021). Assessment of seawater intrusion using ionic ratios: the case of coastal communities along the Central Region of Ghana. *Environmental Earth Sciences.* 80,307.
- Ayeta, E.G., Yafetto, L., Lutterodt, G., Ogbonna, J.F. & Miyittah, M. (2024). Groundwater governance and a snapshot of associated issues in selected coastal communities in Ghana. *Groundwater for Sustainable Development*, 25, 101164.
- Basack, S., Loganathan, M. K., Goswami, G., & Khabbaz, H. (2022). Saltwater Intrusion into Coastal aquifers and associated Risk Management. *Journal of Coastal Research.* 38, 654-672.
- Bhagat, C., Puri, M., Mohapatra, P.K., & Kumar, M. (2021). Imprints of seawater intrusion on groundwater quality and evolution in the coastal districts of south Gujarat, India . *Case Studies in Chemical and Environmental Engineering* 3, 100101.
- Boumaiza, L., Ammar, S.B., Chesnaux, R., Stotler, R.L., Mayer, B., Huneau, F., Johannesson, K.H., Levison, J., Knöller, K., & Stumpp, C. (2023). Nitrate sources and transformation processes in groundwater of a coastal area experiencing various environmental stressors. *Journal of Environmental Management*, 345,118803.
- Bourjila, A., Dimane, F., Ghalit, M., Hammoudani, Y.E., Taher, M., Achoukhi, I., Kamari, S., Haboubi, K., & Benaabidate, L. (2024). Appraising seawater intrusion in the Moroccan Ghiss-Nekor coastal aquifer: Hydrochemical analysis coupled with GIS-based overlay approach. *Desalination and Water Treatment*, Volume 320, 100612.
- Carol E S & Kruse E E (2012). Hydrochemical characterization of the water resources in the coastal environments of the outer Río de la Plata estuary, Argentina *J. South Am. Earth Sci.* 37, 113–21.
- Carol, E., Kruse, E. & Mas-Pla, J. (2009). Hydrochemical and isotopic evidence of ground water salinization processes on the coastal plain of Samborombón Bay, Argentina *J. Hydrol.* 365, 335–45
- Chadha, D.K. (1999). A proposed new diagram for geochemical classification of natural waters and interpretation of chemical data. *Hydrogeology Journal*, 7,431-439.

- Chae, K.-T., Yun, S.-T., Yun, S.-M., Kim, K.-H., & So, C.-S. (2012). Seawater–freshwater mixing and resulting calcite dissolution: An example from a coastal alluvial aquifer in eastern South Korea. *Hydrol. Sci. J.*, 57, 1672–1683.
- Custodio, E., & Herrera, C. (2000). Use of the ratio Cl/Br as a hydrogeochemical tracer in groundwater hydrology. *Boletín Geológico Y Minero*, 111, 49–67.
- Darko, G., Bi, S., Sarfo, I., Amankwah, S.O.Y., Azeez, F.E., Yeboah, E., Oduro, C., E.A. G., Kedjanyi; Archer, B., & Awuah, A. (2022). Impacts of climate hazards on coastal livelihoods in Ghana: the case of Ningo-Prampram in the Greater Accra region. *Environment, Development and Sustainability*, 24, 1445–1474. doi:10.1007/s10668-021-01492-z.
- Davis, S.N., Fabryka-Martin, J., & Wolfsberg, L.E., (2004). Variations of bromide in potable ground water in the United States. *Ground Water* 42, 902–909.
- Dickson, K.B. & Benneh, G. (1980). “A New Geography of Ghana,” Longman, London.
- El Moujabber, M., Bou Samra, B., Darwish, T., & Atallah T (2006). Comparison of different indicators for groundwater contamination by seawater intrusion on the Lebanese coast *Water Resour. Manag.* 20 161–8
- Errich, A., El Hajjaji, S., Fekhaoui, M., Hammouti, B., Azzoui, K., Lamhamdi, A., & Jodeh, S. (2023). *et al.* Seawater Intrusion and Nitrate Contamination in the Fum Al Wad Coastal Plain, South Morocco. *J. Earth Sci.* 34, 1940–1950.
- Fitzgerald, J.W., (1991). Marine aerosols: a review. *Atmospheric Environment* 25A, 533–545.
- Foppen, J.W.A., Lutterodt, G., Rau, G.C., and Minkah, O (2020). Groundwater flow system analysis in the regolith of Dodowa on the Accra Plains, Ghana *Journal of Hydrology: Regional Studies*, 28, 100663.
- Gaillardet, J., Dupre, B., Louvat, P., & Allegre, C.J. (1999). Global silicate weathering and CO consumption rates deduced from the chemistry of large rivers. *Chemical Geology* 159 3–30.
- Ganyaglo, S.Y., Osa, S., Akiti, T., Armah, T., Gourcy, L., Vitvar, T., & Otoo, I.A. (2017). Application of geochemical and stable isotopic tracers to investigate groundwater salinity in the Ochi-Narkwa Basin, Ghana. *Hydrol. Sci. J.* 62 (8), 1301–1316.
- Ghana Statistical Service (2014). 2010 Population and housing Census. Analytical Report. Ningo Prampram Municipality [Ningo Prampram.pdf](https://statsghana.gov.gh/Ningo_Prampram.pdf) (statsghana.gov.gh).
- Gong, S.L., Barrie, L.A., & Blanchet, J.P., (1997). Modelling sea-salt aerosols in the atmosphere—1. Model development. *Journal of Geophysical Research*, 102, 3805–3818.
- Grant, G., Oteng-Ababio, M., & Sivilien, J. (2019). Greater Accra’s new urban extension at Ningo-Prampram: urban promise or urban peril? *International Planning Studies*, 24, 325–340.
- Idowu, T.E., & Lasisi, K.H. (2020). Seawater intrusion in the coastal aquifers of East and Horn of Africa: A review from a regional perspective. *Scientific African*, 8, e00402.
- Jampani, M., Liedl, R., Hülsmann, S., Sonkamble, S., & Amerasinghe, P. (2020). Hydrogeochemical and mixing processes controlling groundwater chemistry in a wastewater irrigated agricultural system of India. *Chemosphere*, 239, 124741.
- Jeen, S-W., Kang, J., Jung, H., & Lee, J.(2021). Review of Seawater Intrusion in Western Coastal Regions of South Korea. *Water*, 13, 761.



- Jena, M.R., Tripathy, J.K., Sahoo, D., & Sahu, P. (2024). Geochemical Evaluation of Groundwater Quality in the Coastal Aquifers of Kujang Block, Jagatsinghpur District, Eastern Odisha, India *Water Air Soil Pollut.*, 235, 349.
- Junner, N. R., & Bates, D. A. (1945). Reports on the geology and hydrology of the coastal area east of the Akwapim Range. Government Printing Department.
- Kesse, G. O. (1985). The mineral and rock resources of Ghana. Balkema, Rotterdam, 32-41.
- Klassen, J., & Allen, D.M. (2017) Assessing the risk of saltwater intrusion in coastal aquifers. *J Hydrol* 551, 730–745.
- Klassen, J., Allen, D. M., & Kirste, D. (2014). Chemical Indicators of Saltwater Intrusion for the Gulf Islands, British Columbia. Final Report. Simon Fraser University
- Kortatsi, B.K., & Jørgensen, N.O., (2001). The origin of high salinity waters in the accra plains groundwaters. In: *Proceedings of the First International Conference on Saltwater Intrusion and Coastal Aquifers - Monitoring, Modeling, and Management*. Essaouira, Morocco, 23–25 April.
- Kortatsi, B.K., (2006). Hydrochemical characterization of groundwater in the Accra plains of Ghana. *Environ. Geol.* 50, 299–311.
- Kummu, M., de Moel, H., Salvucci, G., Viviroli, D., Ward, P.J., & Varis, O. (2016). Over the hills and further away from coast: Global geospatial patterns of human and environment over the 20th–21st centuries. *Environmental Research Letters* 11, 034010.
- Lee, J.-Y., & Song, S.-H. (2007). Groundwater chemistry and ionic ratios in a western coastal aquifer of Buan, Korea: Implication for sea water intrusion. *Geosci. J.* 2007, 11, 259–270.
- Li, C., Gao, X., Li, S., & Bundschuh J.(2020). A review of the distribution, sources, genesis, and environmental concerns of salinity in groundwater. *Environ Sci Pollut Res Int.*, 27, 41157-41174.
- Lutterodt, G., Miyittah, M.K., Addy, B., Ansa, E.D.O., & Takase, M. (2021) Groundwater pollution assessment in a coastal aquifer in Cape Coast, Ghana. *Heliyon*, 7 4e06751.
- MacManus, K, Balk, D, Engin, H, McGranahan, G & Inman, R (2021). Estimating population and urban areas at risk of coastal hazards, 1990–2015: How data choices matter. *Earth System Science Data*, 13, 5747–5801.
- Macrae, M.L., Devito, K.J., Strack, M. & Waddington, J.M. (2013). Effect of water table drawdown on peatland nutrient dynamics: implications for climate change. *Biogeochemistry*, 112, 661–676.
- Mahmoudi, N., Nakhaei, M., & Porhemmat, J. (2017) Assessment of hydrogeochemistry and contamination of Varamin deep aquifer, Tehran Province, Iran *Environ Earth Sci*, 76, 370.
- Malki, M., Bouchaou, L., Hirich, A., Brahim, A.Y., & Choukr-Allah, R. (2017). Impact of agricultural practices on groundwater quality in intensive irrigated area of Chtouka-Massa, Morocco. *Science of The Total Environmen.*, 574, 760-770.
- Manivannan, V., & Elango, L. (2019) Seawater intrusion and submarine groundwater discharge along the Indian coast. *Environ Sci Pollut Res* 26, 31592–31608.
- Maul, G.A., & Duedall, I.W. (2019). Demography of Coastal Populations. In: Finkl, C.W., Makowski, C. (eds) *Encyclopedia of Coastal Science. Encyclopedia of Earth Sciences Series*. Springer, Cham. Mkilima, T.

- (2023) Groundwater salinity and irrigation suitability in low-lying coastal areas. A case of Dar es Salaam, Tanzania. *Watershed Ecology and the Environment* 5, 173-185.
- Moorthy, P., Sundaramoorthy, S., Roy, P.D., Jonathan, M.P., Tune Usha, T., Gowrappan, M., & Chokkalingam, L. (2024). Identifying seawater interaction with coastal aquifers using hydrochemical and GIS for Nagapattinam district, southeast coast of India. *Desalination and Water Treatment*, 320, 100703.
- Motevalli, A., Moradi H.R., & Javadi, S. (2018). A comprehensive evaluation of groundwater vulnerability to saltwater up-coning and sea water intrusion in a coastal aquifer (case study: Ghaemshahr-juybar aquifer). *J Hydrol Hydromech* 557,753–773.
- Nair, I. S., Brindha, K., & Elango, L. (2016). Identification of salinization by bromide and fluoride concentration in coastal aquifers near Chennai, southern India. *Water Science*, 30, 41-50
- Nair, I. S., Brindha, K., & Elango, L. (2020). Assessing the origin and processes controlling groundwater salinization in coastal aquifers through integrated hydrochemical, isotopic and Hydrogeochemical modelling techniques. *Hydrological Sciences Journal*, 66, 152–164.
- Narvaez-Montoya, C., Mählknecht, J., Torres-Martínez, J.A., Mora, A., & Bertrand, G. (2023). Seawater intrusion pattern recognition supported by unsupervised learning: A systematic, review and application. *Science of The Total Environment*, 864,160933.
- Ndoye, S., Fontaine, C., Gaye, C. B., & Razack, M. (2018). Groundwater quality and suitability for different uses in the saloum area of Senegal. *Water* 10, 1837.
- Neumann B, Vafeidis A.T., Zimmermann J, and & Nicholls R. J. (2015). Future coastal population growth and exposure to sea-level rise and coastal flooding--a global assessment. *PLoS One*. 11; 10 (3):e0118571. doi: 10.1371/journal.pone.0118571. Erratum in: *PLoS One*. 2015; 10(6):e0131375. PMID: 25760037; PMCID: PMC4367969.
- Ningo-Prampam District Assembly (2023). Republic of Ghana Composite Budget for 2023-2026 Program based budget estimates for Ningo-Prampam District Assembly. Minist
- Obeng, P.A., Keraita, B., Oduro-Kwarteng, S., Bregnhøj, H., Abaidoo, R.C., Awuah, E., & Konradsen, F. (2015). Usage and Barriers to Use of Latrines in a Ghanaian Peri-Urban Community. *Environ. Process*. 2, 261–274.
- Osiakwan, G. M., Appiah-Adjei, E. K., Kabo-Bah, A. T., Gibrilla, A., & Anornu, G. (2021). Assessment of groundwater quality and the controlling factors in coastal aquifers of Ghana: An integrated statistical, geostatistical and hydrogeochemical approach. *Journal of African Earth Sciences*, 184, 104371.
- Ostad-Ali-Askari, K., Kharazi, H.G., Shayannejad, M., & Zareian, M.J. (2019). Effect of management strategies on reducing negative impacts of climate change on water resources of the Isfahan–Borkhar aquifer using MODFLOW. *River Research and Applications*. 35, 611–631.
- Ouhamdouch, S., Bahir, M., & Ouazar, D.(2021). Seawater intrusion into coastal aquifers from semi-arid environments, Case of the alluvial aquifer of Essaouira basin (Morocco) *Carbonates Evaporites*., 36, 5.
- Park Seh-Chang, Yun, Seong-Taek, Chae, Gi-Tak, Yoo, In-Sik, Shin, Kwang-Sub, Heo, Chul-Ho, & Lee, Sang-Kyu

- (2005). Regional hydrochemical study on salinization of coastal aquifers, western coastal area of South Korea. *J Hydrol*, 313,182–194
- Park, Y., Lee, J.Y., Kim, J.H., and & Song, S.H. (2012). National scale evaluation of groundwater chemistry in Korea coastal aquifers: evidences of seawater intrusion. *Environ Earth Sci.*, 66, 707–718.
- Piper A. M. (1944). A graphic procedure for the geo-chemical interpretation of water analysis. *USGS Groundwater. eos, Transactions American Geophysical Union*: 25, 914-928.
- Prusty, S., & Farooq, S.H. (2020). Seawater intrusion in the coastal aquifers of India - A review. *HydroResearch*, 3, 61–74.
- Pulido-Leboeuf, P., Pulido-Bosch A., Ml C., Vallejos A., & Andreu J.M. (2003). Strontium,  $\text{SO}_4/\text{Cl}$  and  $\text{Mg}/\text{Ca}$  ratios as tracers for the evolution of seawater into coastal aquifers: The example of Castell de Ferro-aquifer. *CR Geosci.*, 335,1039–1048.
- Rabinove C. J., Long Ford R. H., & BrookHart J. W. (1958)Saline water resource of North Dakota. U.S. Geological. Survey Water-Supply Paper, 1428, 72.
- Raja, P., Krishnaraj, S., Selvaraj, G., Kumar, S. and & Francis, V. (2021). Hydrogeochemical investigations to assess groundwater and saline water interaction in coastal aquifers of the southeast coast, Tamil Nadu, India. *Environ Sci Pollut Res* 28, 5495–5519.
- Rajendiran, T., . Sabarathinam, C., Chandrasekar, T., Panda, B., . Mathivanan, M., 4 Nagappan, G., Natesan, D., Ghai, M., Singh, D.K., & Alagappan, R.(2021). Geochemical variations due to salinization in groundwater along the southeast coast of India *SN Applied Sciences*, 3:581.
- Rakib, M.A. . Quraishi, S.B., Newaz, M. A., Sultana, J., . Bodrud-Doza, M., Rahman , M.A.,. Patwary, M.A., & Bhuiyan, M.A.H. (2022). Groundwater quality and human health risk assessment in selected coastal and floodplain areas of Bangladesh. *Journal of Contaminant Hydrology*, 249, 104041.
- Revelle, R. (1941). Criteria for recognition of seawater in groundwater. *Trans. Am. Geophys. Union*, 22, 593 597.
- Ruiz-Pico, A., Pérez-Cuenca, A., Serrano-Agila, R., Maza-Criollo, D., Leiva-Piedra, J., & Salazar-Campos, J. (2019). Hydrochemical characterization of groundwater in the Loja Basin (Ecuador), *Applied Geochemistry*, 104, 1-9.
- Salimi, S., Almuktar, S. A., & Scholz, M. (2021). Impact of climate change on wetland ecosystems: A critical review of experimental wetlands. *Journal of Environmental Management*, 286, 112160.
- Sawyer, C., & McCarthy, P. (1967). *Chemistry for Sanitary Engineering*. – McGraw-Hill, New York.
- Scharping R. J., Garman K. M., Henry R. P., Eswara P. J., & Garey J. R. (2018). The fate of urban springs: pumping-induced seawater intrusion in a phreatic cave. *J. Hydrol.*, 564, 230–245.
- Schoeller, H. (1965). Qualitative evaluation of groundwater resources. In: *Methods and techniques of groundwater investigations and development*. UNESCO, 54–83.
- Senthilkumar, M and Gnanasundar, D (2021). Application of  $\text{Cl}/\text{Br}$  ratio to demarcate the fresh-saline water interface in coastal aquifers of northern Tamilnadu, Southern India. *G roundwater for Sustainable Development*, 15, 100658.
- Shaji, E., Santosh, M., Sarath, K.V., Prakash, P., Deepchand, V., & Divya, B.V. (2021). Arsenic contamination of groundwater: A global synopsis

- with focus on the Indian Peninsula. *Geoscience Frontiers*, 12, 3, 101079.
- Shin, K., Koh, D.-C., Jung, H., & Lee, J. (2020). The Hydrogeochemical Characteristics of Groundwater Subjected to Seawater Intrusion in the Archipelago, Korea. *Water* 2020, 12, 1542.
- Sinclair AJ (1974). Selection of thresholds in geochemical data using probability graphs. *J Geochem Explor* 3, 129–149.
- Slama, F., & Bouhlila, R. (2017). Multivariate statistical analysis and Hydrogeochemical modelling of seawater-freshwater mixing along selected flow paths: case of Korba coastal aquifer Tunisia. *Estuar. Coast. Shelf Sci.*, ECSA 55 Unbounded boundaries and shifting baselines: estuaries and coastal seas in a rapidly changing world 198 636e647. <https://doi.org/10.1016/j.ecss.2016.10.005>.
- Sudaryanto & Nailly, W. (2018). Ratio of Major Ions in Groundwater to Determine Saltwater Intrusion in Coastal Areas IOP Conf. Ser.: Earth Environ. Sci. 118 012021.
- Sunkari, E.D., Abu, M., & Zango, M.S. (2021). Geochemical evolution and tracing of groundwater salinization using different ionic ratios, multivariate statistical and geochemical modeling approaches in a typical semi-arid basin. *Journal of Contaminant Hydrology*, 236, 103742.
- Telahigue F., Mejri H., Mansouri B., Souid F., Agoubi B., Chahlaoui A., & Kharroubi, A. (2020a). Assessing seawater intrusion in arid and semi-arid Mediterranean coastal aquifers using geochemical approaches. *Phys. Chem. Earth Parts A/B/C*. 115:102811. doi: 10.1016/j.pce.2019.102811.
- Telahigue, F., Agoubi, B., Souid, F., & Kharroubi, A. (2018b). Assessment of seawater intrusion in an arid coastal aquifer, south-eastern Tunisia, using multivariate statistical analysis and chloride mass balance. *Phys. Chem. Earth, Parts A/B/C*. 106, 37-46.
- Telahigue, F., Agoubi, B., Souid, F., & Kharroubi, A., (2018a). Groundwater chemistry and 32 radon-222 distribution in Jerba Island, Tunisia. *J. Environl. Radioact.* 182, 74-84.
- Telahigue, F., Mejri, H., Mansouri, B., Souid, F., Agoubi, B., Chahlaoui, A., & Kharroubi, A., (2019). Assessing seawater intrusion in arid and semi-arid Mediterranean coastal aquifers using geochemical approaches, *Physics and Chemistry of the Earth*, doi: <https://doi.org/10.1016/j.pce.2019.102811>.
- Telahigue, F., Souid, F., Agoubi, B., Chahlaoui, A., & Kharroubi, A. (2020b). Hydrogeochemical and isotopic evidence of groundwater salinization in a coastal aquifer: A case study in Jerba Island, southeastern Tunisia. *Physics and Chemistry of the Earth, Parts A/B/C*, 118–119, 102886.
- Todd, D.K. (1953). Sea-water intrusion in coastal aquifers, *Eos, Trans. Am. Geophys. Union* 34, 749–754.
- Todd, D.K. (1959). *Ground water hydrology*. United States. John Wiley and Sons. Inc. 277–294.
- Vallejos, A.; Daniele, L.; Sola, F.; Molina, L.; & Pulido-Bosch, A. (2020) Anthropogenic-induced salinization in a dolomite coastal aquifer. *Hydrogeochemical processes. J. Geochem. Explor.* 2020, 209, 106438.
- van Camp, M., Mtoni, Y., I.C. Mjemah, I.C., Bakundukize, C., & Walraevens, K. (2014). Investigating sea-water intrusion due to groundwater pumping with schematic model simulations: the example of the Dar es Salaam coastal aquifer in Tanzania, *J. Afr. Earth Sci.* 96, 71–78.
- Vengosh, A., & Rosenthal, E. (1994) Saline groundwater in Israel: Its bearing on

- the water crisis in the country. *J. Hydrol.*, 1994, *156*, 389–430.
- Venkatramanan, S.,; Chung, S.Y.,; Kim, T.H.,; Prasanna, M.V., & Hamm (2015). S.Y. Assessment and distribution of metals contamination in groundwater: A case study of Busan city, Korea. *Water Qual. Expo. Health* 2015, *7*, 219–225.
- Venkatramanan, S., Chung, S.Y., Selvam, S., Lee, S.Y., & Elzain, H.E. (2017). Factors controlling groundwater quality in the Yeonjegu District of Busan City, Korea, using the hydrogeochemical processes and fuzzy GIS. *Environ. Sci. Pollut. Res.* *24*, 23679–23693.
- Visvalingam, G., Krishnaraj, S., Andiyappan, R.K., Kamalpathy, R., Datchanamourthy, S.V., & Lagudu, S. (2024). Understanding the impact of climate-induced sea level rise on groundwater inundation in a low-lying coastal area: A numerical simulation in Southeast India. *Regional Studies in Marine Science*, *70*, 103401.
- Wang, H., Ni, J., Song, Q., Li, C., Wang, F., & Cao, Y. (2021). Analysis of coastal groundwater hydrochemistry evolution based on groundwater flow system division. *Journal of Hydrology*, *601*, 126631.
- Wen, X., Lu, J., Wu, J., Lin, Y., & Luo, Y. (2019). Influence of coastal groundwater salinization on the distribution and risks of heavy metals Xiaohu. *Science of the Total Environment*, *652*, 267–277.
- Xu, J., Gui, H., Xia, Y., Zhao, H., Li, C., Chen, J., Wang, C., & Chen, C. (2022). Study on hydrogeochemical connection and water quality assessment of subsidence lake and shallow groundwater in Luling coal-mining area of the Huaibei coalfield, Eastern China. *Water Supply*, *22*, 1735–1750.
- Yidana, S.M. & Chegbele, L.P. (2013). The hydraulic conductivity field and groundwater flow in the unconfined aquifer system of the Keta Strip, Ghana. *Journal of African Earth Sciences*, *86*, 45–52.
- Zhang, M., Huang, G., Liu, C., Zhang, Y., Chen, Z & Wang, J. (2020). Distributions and origins of nitrate, nitrite, and ammonium in various aquifers in an urbanized coastal area, south China. *Journal of Hydrology*, *582*, 124528.
- Zhang, T., Wang, P., He, J., Liu, D., Wang, M., Wang, M., & Xia, S. (2023). Hydrochemical Characteristics, Water Quality, and Evolution of Groundwater in Northeast China. *Water*, *15*, 2669.
- Zhang, Y., Li, X., Luo, M., Wei, C., Huang, X., Xiao, Y., Qin, L., & Pei, Q. (2021). Hydrochemistry and Entropy-Based Groundwater Quality Assessment in the Suining Area, Southwestern China. *Hindawi Journal of Chemistry*, 5591892.

## Funding

The work was funded from book and research allowance obtained from the University of Environment and Sustainable development, Somanya.

## Acknowledgements

The author is grateful to Dr. Samuel Ganyaglo, Dr Gibrilla Abass and Mr. Godfred Ayanu all of the National Nuclear Research Institute of the Ghana Atomic Energy Commission, for their help in the analyses of the Chemical Parameters. Sincere thanks go to Field Technicians Mr. Albert Communisto and Mr. Joseph Tei all of Nuumo Consult limited for support in the field.